Faculty of Engineering of University of Porto

# Resveratrol and Grape's Extract-Loaded Solid Lipid Nanoparticles for the Treatment of Parkinson's and Alzheimer's diseases

Ana Maria Gouveia Duarte

Master thesis realized under the
Integrated Master in Bioengineer
Branch of Biomedical Engineer

Advisor: Prof. Dr[a]. Maria do Carmo Pereira
Co-advisor: Dr[a]. Joana Angélica Loureiro

July 2015

# Abstract

Parkinson's disease is a neurologic disease characterized by both motor and non-motor symptoms, but also by nerve cell loss in the brain. A hallmark characteristic of Parkinson's disease is the presence of Lewy bodies which are abnormal aggregates of protein in nerve cells, and which major component is the α-synuclein. It is believed that this protein plays a crucial role in Parkinson's disease development. Alzheimer's disease is the most common cause of dementia in the elderly, affecting more than 24 million people around the globe. The initial symptoms of this disease include loss of memory and orientation, as well the presence of two pathological features: the presence of neurofibrillary tangles and amyloid plaques, which major component is the amyloid-β peptide. Despite the advances in the investigation of new therapies for this disease, current treatment available continues focusing on reducing the symptoms of the patient and not on the reversal of the disease. Moreover, the blood-brain barrier remains the major obstacle to the development of new therapies due to its restrictions, limiting approximately 98% of the small molecules. Through the use of nanoparticles targeted to the brain and where the drug can be encapsulated, the crossing of the blood-brain barrier becomes possible by drugs that otherwise were not able. Therefore, the drug is slowly released in the brain, increasing the efficiency of the therapeutic drug and decreasing peripheral and/or systemic toxicities that could arise from its systemic use.

This study aimed to develop a targeted therapeutic system for intravenous administration, using solid lipid nanoparticles, a biocompatible and biodegradable colloidal delivery system, widely researched for medical applications, with a propose of drug delivery system. The nanoparticles were encapsulated with resveratrol and grape's extracts, the main source of natural resveratrol, to be used as therapeutic agents in the combat against Parkinson's disease and Alzheimer's disease. The lipid nanoparticles were also functionalized with an OX-26 antibody that specifically targets the transferrin. The nanoparticles where characterized morphologically by size, zeta potential and entrapment efficiency. Particle size was in the desired range (150-200nm), their entrapment efficiency percentage achieved the 90%, but the zeta potential was lower than expected, still the nanoparticles remain stable for at least 2 months. When conjugated with the antibodies, the nanoparticles lost their stability, aggregating and resulting in a higher nanoparticle size.

Furthermore, nanoparticle morphology was analysed by transmission electron microscopy, allowing the observation of the spherical shape of the nanoparticles, but also small aggregates in some of the samples. The interaction with α-synuclein and amyloid-β peptides

was also studied with Thioflavin T fluorescent assays and the ability of delaying the aggregation of these peptides could be confirmed, demonstrating that the nanoparticles synthesized are promising candidates for the treatment of both Parkinson's and Alzheimer's disease.

# Resumo

A doença de Parkinson é uma doença neurológica caracterizada tanto por sintomas motores como não motores, mas também pela perda de células nervosas no cérebro. A característica principal desta doença é a presença de corpos *Lewy* que são agregados anormais de proteínas nas células nervosas, e cujo principal componente é a α-sinucleína. Pensa-se que esta proteína desempenha um papel crucial no desenvolvimento da doença de Parkinson. A doença de Alzheimer é a causa mais comum de demência na idade avançada, afetando mais de 24 milhões de pessoas em todo o mundo. Os sintomas iniciais da doença incluem perda de memória e dificuldade na orientação, bem como a presença de duas características patológicas: a presença de emaranhados neurofibrilares e placas de amilóide, cujo principal componente é a amilóide-β. Apesar dos avanços na investigação de novas terapias, os tratamentos atuais continuam a focar-se na redução dos sintomas do paciente e não na reversão da doença. Além disso, a barreira hematoencefálica continua a ser o maior obstáculo ao desenvolvimento de novas terapias devido às suas características limitantes, bloqueando aproximadamente 98% das moléculas pequenas. Através do uso de nanopartículas direcionadas para o cérebro onde o fármaco possa ser encapsulado, a passagem através da barreira hematoencefálica torna-se possível para fármacos que de outra forma não seriam capazes de o fazer. Desta forma, o fármaco é libertado lentamente no cérebro, aumentando a sua eficiência e diminuindo efeitos tóxicos periféricos e/ou sistémicos que poderiam ocorrer do seu uso sistémico.

Este estudo teve como objetivo o desenvolvimento de um sistema terapêutico direcionado para administração intravenosa utilizando nanopartículas lipídicas sólidas, que consiste num sistema coloidal biocompatível e biodegradável de entrega de fármacos e que é amplamente estudado para aplicações médicas com o objetivo de entregar fármacos. Resveratrol e extratos de uva, a fonte natural principal de resveratrol, foram encapsulados nestas nanopartículas para serem utilizados como agentes terapêuticos no combate contra as doenças de Parkinson e Alzheimer. As partículas foram também funcionalizadas com o anticorpo OX-26 que se liga especificamente à transferrina. As nanopartículas foram caracterizadas morfologicamente pelo tamanho, potencial zeta e eficiência de encapsulamento. O tamanho das nanopartículas estava dentro da escala desejada (150-200 nm) e a sua eficiência de encapsulação alcançou os 90%, mas o seu potencial zeta foi mais baixo que o esperado, mas mesmo assim, as partículas continuaram estáveis pelo menos durante 2 meses. Quando conjugadas com os anticorpos, as nanopartículas a sua estabilidade diminuiu, agregando e resultando em nanopartículas de maior tamanho.

Além disso, a morfologia das nanopartículas foi analisada por microscopia eletrónica de transmissão, permitindo a observação da sua forma esférica, mas também de pequenos agregados em algumas amostras. A interação com os péptidos α-sinucleína e amilóide-β foi estudada com ensaios de fluorescência de Tioflavina T e a capacidade de atrasar a agregação destes péptidos foi confirmada, demonstrando que as nanopartículas sintetizadas são candidatos promissores para o tratamento das doenças de Parkinson e Alzheimer.

# Acknowledgments

I would like to express my gratitude to both Prof. Drª. Maria do Carmo Pereira and Drª. Joana Angélica Loureiro for giving me the opportunity to work with their research group and for their constant support, scientific guidance and availability during the thesis research and experimental work. I also want to thank to remaining members of the group for their assistant and welcoming attitude.

I wish to acknowledge to Prof. Drª. Salette Reis for the opportunity to performing some experiments in her laboratory (at Faculty of Pharmacy, University of Porto), but especially to Joana Queiroz and Ana Neves for the support and lessons that they gave me during my time there.

I also would like to give a special thank you to parents and friends for their continuous support and encouragement during not only the development of this thesis but also during the last years.

This work was financially supported by: Project UID/EQU/00511/2013-LEPABE, by the FCT/MEC with national funds and when applicable co-funded by FEDER in the scope of the P2020 Partnership Agreement.

# Contents

# List of figures

# List of tables

# Abbreviations and Symbols

List of abbreviations

| | |
|---|---|
| A30P | Alanine to proline substitution at the position 30 |
| A53T | Alanine to threonine substitution at the position 53 |
| ABC | ATP-binding cassette |
| AD | Alzheimer's disease |
| AMT | Adsorptive-mediated trancytosis |
| ApoE4 | Apolipoprotein genotype |
| APP | Amyloid precursor protein |
| BBB | Blood-brain barrier |
| BDNF | Brain-derived neurotrophic factor |
| BSA | Bovine serum albumin |
| COMT | Catechol-o-methyl-transferase |
| CNS | Central nervous system |
| CSF | Cerebrospinal fluid |
| DA | Dopamine |
| DLS | Dynamic light scattering |
| E46K | Glutamate to lysine substitution at the position 46 |
| EE | Entrapment efficiency |
| EDTA | Ethylenediamine tetraacetic acid |
| ELISA | Enzyme-linked immunosorbent assay |
| FAD | Familial Alzheimer's disease |
| FDA | Food and drug administration |
| GDNF | Glial cell line-derived neurotrophic factor |
| L-dopa | Levodopa |
| MAO B | Monoamine oxidase B |
| NAC | Non-beta-amyloid component |
| P-gp | P-glycoprotein |

| | |
|---|---|
| PD | Parkinson's disease |
| PDI | Polidispersity index |
| PEG | Polyethylene glycol |
| RES | Reticuloendothelial system |
| RMT | Receptor-mediated transcytosis |
| ROS | Reactive oxygen species |
| RPM | Rotation per minute |
| SLN | Solid lipid nanoparticles |
| TEM | Transmission electron microscopy |
| ThT | Thioflavin T |
| UPS | Ubiquitin-dependent proteasome system |
| UV | Ultra-violet |

List of symbols

| | |
|---|---|
| α | Alfa |
| β | Beta |
| γ | Gama |
| nm | Nanometres |
| μL | Microliters |
| μm | Micrometres |
| Da | Daltons |

# Chapter 1

# Introduction

## 1.1 - Motivation

Over the last years, the world's population has been aging at an accelerating rate. Combining this with the increase of the life expectancy in industrialized countries, it is possible to understand the burden of neurodegenerative diseases today.

Parkinson's disease (PD) is the second most common neurodegenerative disorder [1]. It is characterized by both motor and non-motor symptoms, but also by nerve cell loss in the brain. A hallmark characteristic of Parkinson's disease is the presence of Lewy bodies which are abnormal aggregates of protein in nerve cells, and which major component is the α-synuclein [2]. It is believed that this protein plays a crucial role in Parkinson's disease development. Another neurodegenerative disease is the Alzheimer's disease (AD), the most common cause of dementia in the elderly, affecting more than 24 million people around the globe. As PD, the most influential risk factor is the age. The initial symptoms of AD involve loss of memory and orientation, as well the presence of two pathological features: the presence of neurofibrillary tangles and amyloid plaques, which major component is the amyloid-β peptide [3].

Even though the advances in the investigation of new therapies for PD and AD, current treatments available continues focusing on reducing the symptoms of the patient and not on the reversal of the disease. One factor for this to happen it the existence of the blood-brain barrier (BBB), which is responsible for the restriction of the majority of therapeutic drugs, when intravenously administrated, to the central nervous system (CNS). It is also responsible for the dropout of relatively new drugs that have a good efficacy *in vitro* but cannot pass this strict barrier [4].

Nanomedicine was born from the fusion of nanotechnology with the need of drug delivery and studies how the drug administration, pharmacokinetics and pharmacodynamics are affected by the use of nano-sized materials [5]. The role of nanotechnology in the treatment of neurodegerative disease arises from the necessity to mask the physicochemical properties of the therapeutic drugs in order to have a longer blood-stream life and to be able to cross the BBB into the CNS. This can be achieved by encapsulation of the drug in a nanoparticle which can be made of different kinds of biomaterials. Lipid and polymeric nanoparticles are the two most used classes of nanoparticles used for drug delivery across the BBB, due to their

ability to reduce the common side effects of the current drugs through their encapsulation [4].

## 1.2 - Main objective

In this context, the aim of the present work is to develop lipid nanoparticles loaded with therapeutic compounds for the treatment of PD and AD. The therapeutic compound chosen was the resveratrol, which is a biologically active substance found in plants and exhibits several health beneficial effects. One of these effects is neuroprotection in neurodegenerative disease, such as PD and AD [6]. Since it is present mainly in grapes, its extracts are a natural alternative to resveratrol, so they were also encapsulated into lipid nanoparticles.

## 1.3 - Thesis organization

The present dissertation is organized into five different chapters. The first chapter is the *Introduction*, and it is where the motivation and main objective of this research work are stated. The second chapter, *State of the art*, carries out an overview of the Parkinson's and Alzheimer's disease, the blood brain barrier and lipid nanoparticles, and also a review of the last studies on nanoparticles used for the treatment of both Parkinson's disease and Alzheimer's disease. The *Materials and Methods* chapter describes the list of materials used and all the methodologies applied during this work. Results and respective discussion are described in the Results and Discussion chapter. The last chapter, *Concluding Remarks and Future Perspectives* summarizes the work developed, presenting the main conclusions based on the results obtained, but also suggestions of possible future work that can be useful for the present project. Finally, in the *Annex* are included all the supplementary results.

# Chapter 2

# State of the Art

## 2.1 - Parkinson's disease

Parkinson's disease (PD) is the second most common neurodegenerative disorder, after Alzheimer's disease. It is estimated to affect 10-18% of the world population and has an annual incidence of 0.4-2%. There is also a rising prevalence with age and a higher incidence in the male population [1]. PD is an incurable and progressive disorder that is characterized by a chronic and progressive movement disorder with pigmented neuron degeneration in the *substantia nigra*, resulting in a decrease in nigrostriatal availability of the neurotransmitter dopamine [7]. In most cases, PD occurs as a sporadic type of disease (90-95%) with no apparent genetic linkage, but can also appear as a rare familial form (5-10%) [8, 9]. The average age of disease onset in PD is around 60 years, with a life expectancy of about 15 years since diagnosis. Furthermore, the majority of early-onset patients (diagnosed under 40 years old) have a positive family history of PD and long disease duration, while older patients (over the age of 70 years) tend to have shorter disease durations ( approximately 5 to 10 years) and more rapid and severe disease progression [10, 11].

PD has two main neuropathological hallmarks. The first one is the degeneration of basal ganglia neurons, predominantly pigmented dopaminergic neurons of the *substantia nigra* pars compact of the midbrain [12, 13], and the second is the presence of α-synuclein positive intracytoplasmatic inclusions and axons known as Lewy bodies and Lewy neurites that are formed in the survival dopaminergic neurons [14]. Lewy bodies are cytoplasmic inclusions constituted by aggregated proteins. As mentioned before, the major component of Lewy bodies in sporadic PD is the α-synuclein, a 140 amino acid presynaptic protein. It is thought that this protein plays a crucial role in PD development [15]. Moreover, examination of PD brains identified the presence of neurofilaments and ubiquitin, changes in mitochondrial function, increased oxidative stress, lysosomal dysfunction, protein aggregation and impaired degradation, deposition of iron as well inflammation and glial activation [16, 17].

Until a few years ago, the aggregation of α-synuclein protein was thought to be modulated by point mutations associated with familial PD, various environmental factors, posttranslational modifications, and interaction with cellular membranes and different proteins [18]. Nevertheless, it was not known if genetic or epigenetic factors might perturb the metabolism, solubility, or interactions of the α-synuclein in sporadic PD and synuclein in

dystrophic neurites [13]. Nowadays, PD is considered to have a complex multi-hit etiology involving multiple influences including lifestyle, genetics (e.g. α-synuclein mutations) and environment (e.g. insecticide exposure) [19, 20]. In 2007, a dual-hit hypothesis for the progression of PD was proposed, suggesting that an external factor could initiate this pathogenesis by induction of the α-synuclein pathology, which moves along two potential paths to the midbrain. One of these paths begins due to the exposure in the olfactory bulb, while the other is caused by the exposure in the gastrointestinal tract. At some point, both of these pathways result in damage to the nervous system [21]. The progression of the PD is hypothesized to occur in a predictable pattern that begins in the caudal brainstem (dorsal motor nucleus of glossopharyngeal and vagal nerves) and olfactory bulb (anterior olfactory nucleus) (stage I), ascending to the pontine tegmentum (stage II), midbrain (stage III), mesocortex and allocortex (stage IV) and finally culminating in widespread neocortical involvement (stages V and VI) [22]. This progression is represented in Table 2.1.

**Table 2.1 -** Parkinson's disease stages by Braak (I to VI), and respective pathological disease's progress and symptoms (emphasis on non-motor symptoms). Adapted from [23].

| Stage | I | II | III | | IV | V and VI |
|---|---|---|---|---|---|---|
| **Pathology** | Enteric plexus, olfactory bulb, vagus nerve, cardiac sympathetic neurons, parasympathetic cholinergic dysfunction | Locus coeruleus, reticular formation | Amygdala, Meynert's nucleus | Substantia nigra | Temporal mesocortex, allocortex, limbic circuit | Widespread neocortical involvement |
| **Symptoms** | Constipation, dysautonomia, hyposmia, anxiety, urinary and erectile dysfunction | Sleep disturbances, depression | Unilateral tremor and bradykinesia, subclinical gait dysfunction, behavioural memory disorder | | Impulse control disorders, memory and emotional impairment | Motor symptoms |

## 2.2.1 - α-Synuclein and Parkinson's disease

The α-synuclein protein is encoded by a single gene, the SNCA gene, which consists on seven exons located at the chromosome 4, and lacks both cysteine and tryptophan residues [18, 19]. Moreover the α-synuclein protein is small, soluble and highly conserved, with the predominant isoform being 140 amino acids long [24].

In 1997, after a mutation in α-synuclein gene was found to be associated with the familial cases of early-onset PD, and its aggregates were found to accumulate in components of the neural perikaryal (Lewy bodies) and neuronal processes (Lewy neuritis), the interest of study this protein increased [18, 25].

A major effect of the α-synuclein mutation that leads to an alanine to threonine substitution at position 53 (A53T), is thought to be the promotion of the aggregation of α-synuclein into fibrillar assemblies in nerve cells [13], resulting in the formation of Lewy bodies and Lewy neurites [26]. Due to this, the α-synuclein aggregation and Lewy bodies' formation could be important in the etiology and pathogenesis of all cases of PD [13, 16].

The abnormal accumulation of α-synuclein insoluble aggregates in neuronal cells that characterizes PD, is also related with other neurodegenerative conditions which are collectively termed as synucleinopathies, such as dementia with Lewy bodies and multiple system atrophy, as well as rare disorders such as various neuroaxonal dystrophies [11, 27].

## Localization of α-synuclein

α-Synuclein in its native, aggregated and supposed pathological (oligomeric, phosphorylated) form has been found in a variety of tissues from both living and deceased PD patients including cerebrospinal fluid (CSF), blood (erythrocytes and platelets), urine, saliva, gastrointestinal tract, vagus nerve, sympathetic and stellate ganglia, cutaneous autonomic nerves, and submandibular gland [19, 24, 28].

Thus, this protein is abundantly expressed in the nervous system, comprising 1% of total cytosolic protein. In presynaptic terminals α-synuclein is present in high concentration in close proximity, but no within, synaptic vesicles, and it is found in both soluble and membrane-associated fractions of the brain [29].

## Structural properties and function of α-synuclein

The α-synuclein protein, in aqueous solution, does not have a defined structure, being an intrinsically disordered protein (hence the term *natively unfolded protein*) at neutral pH, but compacter than a random coil (Figure 2.1: left image). The intrinsically disordered proteins are characterized by a unique combination of low overall hydrophobicity, low sequence complexity and high net charge. Thus existing as dynamic and highly flexible structural ensembles, either at the secondary or at the tertiary structure level [18].

The structure of α-synuclein (Figure 2.1: right image) can be divided into three different regions: an amino terminus (residues 1–60) which contain four 11-amino acid imperfect repeats (coding for amphipathic α-helices) with a conserved motif (KTKEGV), a central hydrophobic region (residues 61–95), containing the hydrophobic and highly amyloidogenic Non-beta-amyloid component (NAC) region and three additional KTKEGV repeats, which confers the β-sheet potential, and finally, a carboxyl terminus (residues 96–140), containing the highly enriched in acidic residues and the prolines C-terminal region, that confers an highly negative charge. While, the first two regions comprise a membrane-binding domain, the C-terminal tail is thought to contain protein–protein and protein–small molecule interaction sites [18, 27].

The α-synuclein protein is a member of the synuclein family of proteins, which also include β- and γ-synuclein. What structurally differentiates α-synuclein from the other family members is the NAC region. All three members of the family are predominantly neuronal proteins that under physiological conditions localize preferentially to presynaptic terminals [30].

The α-synuclein might have several functions, which include synaptic vesicle release and trafficking, fatty acid binding and physiological regulation of certain enzymes, transporters,

and neurotransmitter vesicles, as well as roles in neuronal survival. Moreover, α-, β-, and γ-synucleins are important contributors to long-term operation of the nervous system. Furthermore, α-synuclein can interact with at least 30 proteins, having and important role in cell signalling [18].

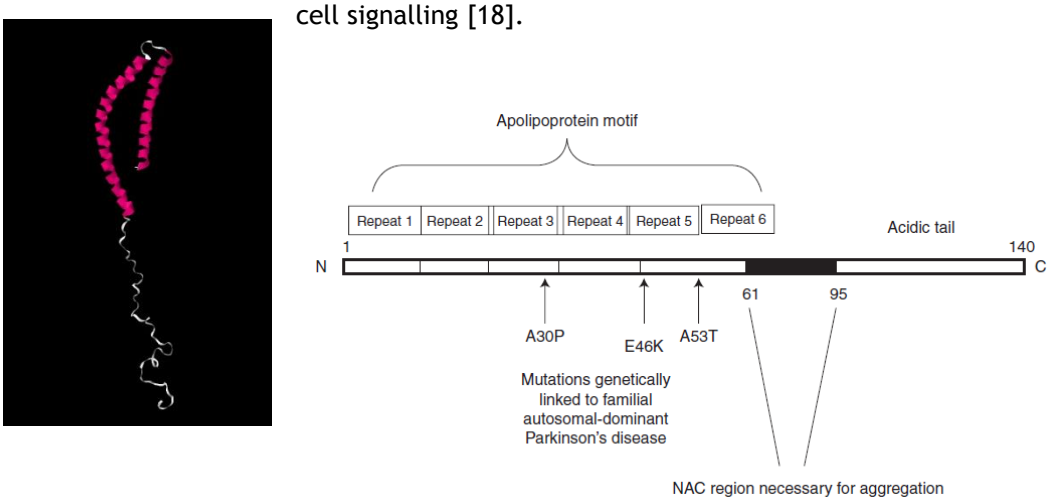


**Figure 2.1** - Representation of the α-synuclein structure taken from the Protein Databank ID: 1XQ8 (left), and schematic structure of α-synuclein protein (right) [27].

## Conformational behaviour of α-synuclein

The α-synuclein protein has the ability to adopt different conformations depending on the environment, and interacts easily with others ligands, such as lipids [31]. Thus, the conformational behaviour of the α-synuclein protein is determined by its relatively low hydrophobicity and high net charge nature. Therefore, alterations in the environment can lead to an increase in its hydrophobicity and/or decrease in the net charge, inducing a partial folding of the protein [18].

As a result, α-synuclein can adopt a number of different conformational states that depends on several conditions and cofactors. These conformational states include the formation of α-helical structures by binding to negatively charged lipids such as phospholipids present on cellular membranes, and it consists in a partially-folded state that is crucial in the aggregation and fibrillation, formation of various oligomeric species, and fibrillar and amorphous aggregates; and of β-sheet-rich structures on prolonged periods of incubation [27].

Furthermore, the partial folding might lead to α-synuclein self-association into amyloidogenic conformations, which is facilitated by the formation of solvent-exposed hydrophobic clusters on the surface of a partially folded protein as a consequence of an increase in concentration, a decrease in pH, an increase in temperature, an addition of amphipathic molecules (e. g. various agrochemicals, such as herbicides or pesticides), an addition of metal ions and other small charged molecules, interaction with charged biopolymers, interaction with other proteins, interaction with membranes, and immersion of a protein into a crowded environment [18].

## Aggregation potential of α-synuclein

The α-synuclein protein forms amyloid fibrils which can be divided in two structural classes: fibrils derived from folded proteins (β-sheet rich), and fibrils derived from

intrinsically disordered proteins. Amyloid fibrils are formed from folded proteins by either the refolding mechanism or by a gain-of-interaction model. In the refolding mechanism, proteins are converted from native structures to fibrils by initially unfolding, and then refolded into a secondary structure that is rich in ß-sheets. The fibrils that are formed in this way are stable due to backbone hydrogen bonding, rather than side chain-side chain interactions. All of these native-like proteins are rich in ß-structure, and as a result form fibrils with minimal alterations to their native structures [18].

The formation of α-synuclein fibrils occurs in a nucleation-dependent manner, where the rate-limiting step is the spontaneous formation of small metastable oligomeric intermediates that results from partial folding and aggregation of unstructured α-synuclein, and exists in rapid equilibrium with its monomeric form. After, fibrils grow by a "dock and lock" mechanism, where monomers initially bind to the exposed regions of a fibril in a reversible manner. This is followed by an irreversible re-organization of the fibril surface, which generates the most optimal surface area for further fibril growth. Thus, the formation of oligomers is also a highly ordered process that involves an intrinsic rate-limiting lag phase. Nevertheless, a wide range of amyloidogenic proteins have been shown to assemble into common oligomeric and fibrillar conformations. This fact suggests that amyloid misfolding is largely mediated by peptidebackbone interactions, and not by interactions of the side groups [18].

The α-synuclein protein aggregation can take place e in the cytoplasm or inside the neurons, in association with the cellular membrane, and it is represented in Figure 2.2.

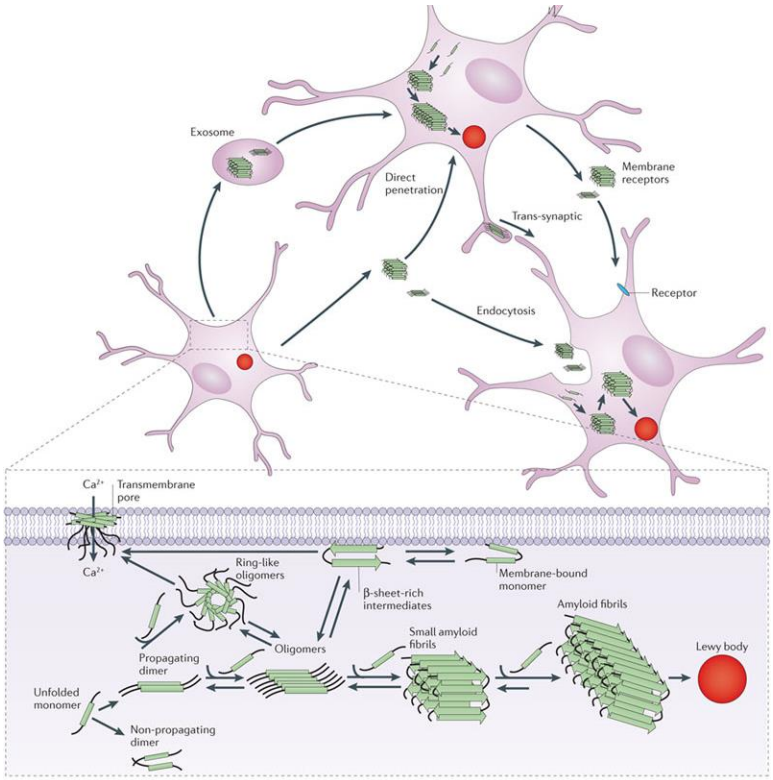


**Figure 2.2** – Mechanisms of α-synuclein aggregation and propagation. Image from [32].

## Structure of the oligomers formed

There is at least three structural classes of amyloid oligomers (prefibrillar, fibrillar and annular) that are formed depending on the environmental conditions. Since α-synuclein belongs to a class of intrinsically disordered amyloid proteins it forms fibrils by converting either all or part of the previously unstructured polypeptide into well-defined, ß-sheet rich secondary structures. The α-synuclein fibrils are composed of several protofilaments containing a cross-ß structure in which ß-strands are arranged in parallel, and the ß-sheets are in-register with highly ordered amino acid side chain patterns exposed on the surface of the ß-sheets. Furthermore, the side-chains protruding from the two ß-sheets of the cross-ß spine interdigitate in a self-complementary manner to give rise to highly ordered structures known as steric zippers [18].

The α-synuclein fibrils can exhibit differences in the structure in consequence of variations in the folding of the ß-sheets, differences in the molecular packing between sheet interfaces, or interactions of side chains with the environment. However, at the molecular level, fibrils and aggregates of α-synuclein have a five-layered parallel, inregister ß-sheets core that consists of a five-layered ß-sandwich [33]. Still, it is not clear whether they are parallel or antiparallel sheets (i.e. the initial α-synuclein oligomers may adopt an antiparallel structure whereas the fibrils are mostly parallel ß-sheets) [34].

The structural of the oligomers is translated to variability in cytotoxicity and biological activity [18]. Moreover, their ability to induce aggregation provides a molecular basis for the heterogeneous group of synucleinopathies caused by α-synuclein aggregation [35].

### Propagation of α-synuclein aggregates

Recent findings hypothesize that amyloids associated with neurodegenerative diseases spread in a prion-like fashion [35]. Similarly to the self-propagating mechanism of infectious prion proteins, misfolded α-synuclein assemblies seed the aggregation of monomeric α-synuclein *in vitro* and spread in a nucleation-dependent seeding mechanism from one cell to another in cell cultures and animal models. Furthermore, Lewy bodies and Lewy neurites have been shown to spread from the brain of patients developing PD to grafted neuronal cells [18]. The mechanism of α-synuclein oligomers and monomers propagation between cells is represented on Figure 2.2 and it can occur via endocytosis, direct penetration, trans-synaptic transmission or through membrane receptor [36]. It has been verified that Lewy bodies and Lewy neurites first appear in the dorsal motor of the vagal nerve in the brainstem and anterior olfactory structures, then spread stereotypically to large parts of the brain, following defined patterns as referred before. Thus, it is considered that the pathology begins first at the olfactory bulb and the dorsal vagal nucleus and gradually follows an ascending course, culminating in widespread α-synuclein pathology at the later stages, involving cortical regions, whereas the *substantia nigra* is only affected in stage 3 of this scheme [22]. Despite this hypothesis does not explain the absence of clinical symptoms in subjects who on autopsy have widespread α-synuclein pathology, it appears to hold up for the majority, but not all, of cases examined [37].

### The potential pathogenic effects of α-synuclein

During the aggregation of the α-synuclein occurs the formation of metastable oligomer intermediates of α-synuclein that are considered to be the disease-associated species of the protein [18]. However, there is some inconsistency about which is the major neurotoxic species, the oligomers and/or the fibrils [18, 38].

There are three major classes of the neurotoxic mechanisms of α-synuclein and its aggregates: mechanical disruption of cellular compartments/processes, toxic gain of function, and toxic loss of function. Permeation of cellular membranes is considered to be the main neurotoxic mechanism, and it is based on the capacity of α-synuclein oligomers binding to lipid membranes and to disrupt membrane bilayers, but also because certain oligomeric forms were shown to penetrate membranes, leading or not to the formation of pore-like channels, and consequently cell death. Moreover, the impairment of α-synuclein degradation via proteasome inhibition by the aggregated species and copper-dependent generation of reactive oxygen species (ROS) have also been proposed as possible neurotoxic mechanisms of the α-synuclein aggregates. It is hypothesized that the α-synuclein-related neurotoxicity might arise from a loss of function [18]. On Figure 2.3 is represented both mechanism of α-synuclein aggregation and toxicity model, where both oligomers and amyloid fibrils contribute to neurotoxicity (e.g. oxidative stress, protein sequestration, disruption of axonal transport, synaptic dysfunction, inhibition of ubiquitin-dependent proteasome (UPS) system and mitochondrial dysfunction). Here it is also represented the control systems (phagosomes, lysosomes and proteasomes) that prevent or reverse protein misfolding or eliminate misfolded proteins which, at some point of the disease, are overwhelmed by α-synuclein oligomers, thus contributing the toxicity effects [38].

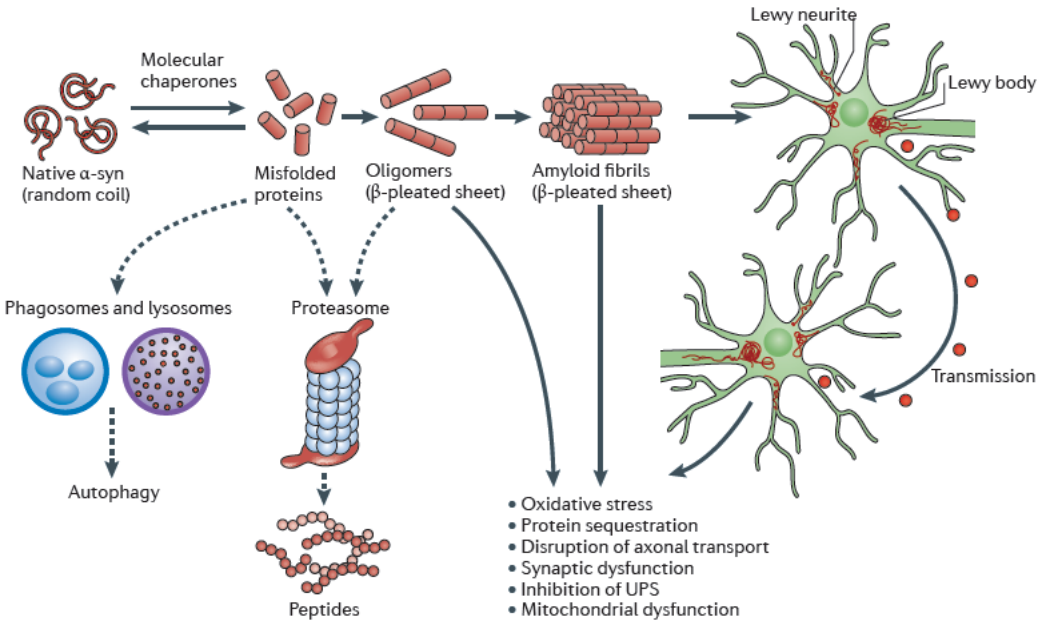


**Figure 2.3** – Mechanism of α-synuclein aggregation and hypothetical model of the α-synuclein toxicity. Image from [38]. UPS: ubiquitin-dependent proteasome system.

## Interaction of α-synuclein with membranes

The α-synuclein protein has several structural features that allows binding with synthetic vesicles containing acidic phospholipids and to cellular membranes. These features comprises several class A2 lipid-binding helices contained in the α-synuclein (distinguished by clustered

basic residues at the polar–apolar interface that are positioned ±100° from the centre of apolar face), a predominance of lysines relative to arginines among the basic residues, and several glutamate residues at the polar surface [18].

In presynaptic termini, monomeric α-synuclein exists in a tightly regulated equilibrium between free and membrane- or vesicle-bound states, being estimated that approximately 15% of α-synuclein is membrane-bound within the synaptic termini. Thus, the inhibition of lipid oxidation by α-synuclein may be a physiological function of the protein [18].

### 2.2.2 - Parkinson's disease-related mutations

There is a small fraction of PD patients who have a familial form of PD with an autosomal-dominant pattern of inheritance. Furthermore, it has been identified three point mutations in the SNCA gene encoding for α-synuclein on patients with familiar PD, leading to A53T, A30P, and E46K amino acid changes (Figure 2.1: right image). These mutations are all associated with autosomal-dominant PD, however, the distribution of the pathology at the cellular and molecular level is different in each case [27].

These three PD-related point mutations do not affect the global structure of human α-synuclein monomer. While the A30P mutation strongly attenuates the helical propensity that is found in the N-terminal region of the wild type α-synuclein, the A53T mutation applies a more modest influence on local structural propensity, resulting in a slightly enhanced preference for extended conformations in a small region around the site of mutation. The E46K mutation resulted in subtle changes in the conformation of the monomeric protein and enhanced the contacts between N- and C-termini of the protein. Moreover, the A30P mutation promoted α-synuclein oligomer formation, while A53T and E46K mutations promoted fibrillation. Thus, all three PD-related mutations of α-synuclein alter its secondary structure and promote its aggregation [18].

### 2.2.3 - Classic Parkinson's disease therapy challenges

Over the years, there has been a massive progress in the treatment of PD, however Levodopa (L-dopa) still is the gold standard for controlling PD symptoms. The therapy of each patient is individualized and several drugs are currently available. Besides L-dopa, there are other compounds that can substitute the L-dopa treatment or be simultaneous administered for an efficient therapy, like dopamine (DA) agonists, catechol-o-methyl-transferase (COMT) inhibitors, nondopaminergic agents, between others.

However, oral L-dopa therapy can be affected by several interfering processes, leading to dose failures and long-term complications. The main situations interfering with the optimal delivery are the necessity to compete with ingested proteins for the amino acid transporters in the gastrointestinal tract and BBB, and the short half-life of L-dopa which is around 36 to 96 minutes. In an advance stage of the disease, this can lead to fluctuating L-dopa concentration levels, and eventually, to fluctuations levels of DA derived from L-dopa. In an attempt to avoid these fluctuations, L-dopa must be administered as multiple doses, however this may not be enough [39]. Furthermore, a continuous intravenous infusion of L-dopa or DA is, at the moment, the only clinical method to abolish the motor fluctuations [40]. But the use of intravenous infusions is not practicable for a chronic therapy [39]. Currently, none of

the available treatments has been able to modify the natural neurodegenerative course of PD [41, 42]. On Table 2.2 are represented the main current drugs used for PD therapy, their clinical use as a monotherapy or adjuvant therapy and their advantages and disadvantages.

Recent studies are focused on optimizing the delivery of L-dopa and other therapeutic drugs so the treatment of PD can be more efficient (more details in the further chapters). These studies are investigating how the BBB compromises the PD treatment and new drug delivery methods [7, 43].

Two examples of new therapeutic compounds are the glial-derived neurotrophic factor (GDNF) and the urocortin. Both have a potential role in the PD treatment due to their neuroprotective and cytoprotectant effect, respectively. However, they have poor penetration of BBB and rapid blood clearance [44].

**Table 2.2** – Current therapeutic approaches used in clinical [45].

| Drug Class | Drug Name | Clinical Use | Advantages | Disadvantages |
|---|---|---|---|---|
| **Levodopa** | Sinemet, Parcopa, Atamet | Monotherapy | Increase levels of endogenous DA | Motor fluctuations, dyskinesias |
| **Continuous Levodopa** | Intravenous bolus, Intravenous infusion, Intestinal L-dopa gel | Monotherapy | Decrease pulsatile DA levels, increase control *on/off* periods, decrease dyskinesia severity and duration, decrease non-motor symptoms | Large volumes required (intravenous), requires surgery and prosthetic device, mechanical problems |
| **Dopamine Agonists** | Piridedil, Pramipexole, Ropinirole, Rotigotine, Cabergoline, Pergolide Bromocriptine | Monotherapy (on young patients), adjuvant therapy | Increase levels of endogenous DA, decrease motor symptoms in early stages of disease | Sedation, impulse control disorder, somnolence, edema |
| **MAO B Inhibitors** | Rasagiline, Selegiline, Safinamide | Initial monotherapy, adjuvant therapy | Well tolerated, decrease catabolism of DA | Mild nausea, constipation, confusion |
| **COMT Inhibitors** | Entacapone, Tolcapone | Adjuvant therapy | Decrease metabolism of L-dopa, decrease in daily dose of L-dopa required, increase daily *on* time | Dyskinesias, diarrhea, hepatic toxicity, dizziness, insomnia, nausea |

## 2.2 - Alzheimer's disease

Alzheimer's disease (AD) is classified as the most common form of dementia, accounting with more than 80% of dementia cases worldwide [46]. The initial symptoms of AD are barely imperceptible since it is characterized by impaired short term memory and difficulties in acquiring new information [47]. As time goes by, the patient starts losing some cognitive functions, exhibit special disorientation and apathy and demonstrates difficulties in performing daily-basic activities, such as walking and dressing up. At the end, the patient experiences intense memory and cognition losses, leading to the immobility of the patient, who eventually succumb to respiratory difficulties (4-6 years after the initial diagnosis) [48].

The advanced age is the major risk factor for developing AD, however the disease can also occur in very rare patients with 20-30 years old who have genetic mutations resulting in the formation of abnormal amyloid precursor protein (APP), presenilin 1, and presenilin 2 genes. Other factors that can influence the occurring of sporadic late-onset AD include mitochondrial defects, apolipoprotein genotype (ApoE4), insulin-dependent diabetes, environmental conditions, and diet [49, 50].

The pathophysiological hallmarks that characterize AD are the presence of neurofibrillary tangles of hyperphosphorylated tau proteins and extracellular amyloid-ß plaques (senile plaques) in the cortex and hippocampus, which are important areas for memory and learning [51]. Anatomically, AD begins in the entorhinal cortex of the brain and progresses to the hippocampus, posterior temporal and parietal neocortex, culminating with diffuse atrophy through the cerebral cortex due to the loss of neurons [50].

## 2.3.1 - Amyloid-ß and Alzheimer's disease

Amyloid-ß is a 4 kDa amphiphilic peptide of 39 to 43 amino acids residues long and it is encoded by a gene localizes in chromosome 21 [52]. In AD patient's brains, amyloid-ß peptide is in a fibrillary state organized in a ß-sheet structure and it is the main constituent of the plaque deposits, extracellular deposits of fibrils and amorphous aggregates of amyloid-ß [53]. Moreover, there is evidence that the concentration amyloid-ß aggregates has a direct relation with the degree of dementia of patients [54]. It is known that amyloid-ß is localized in compartmental cellular organelles such as the endoplasmic reticulum and lysosomal network, however it has also been localized in the cytoplasm of brains of AD patients [55].

Amyloid-ß derives from the APP by sequential activities of ß- and γ-secretases, and it is explained by the cascade hypothesis (Figure 2.4) [56]. The final products of this cascade are two sequences with a length of 40 or 42 amino acids [57]. Usually, the first one is produced more abundantly by cells and its aggregation kinetic rate is much lower than the other (amyloid-$ß_{(1-40)}$ at 20 μM is stable for 8 days or more whereas amyloid-$ß_{(1-42)}$ aggregates immediately) [58, 59]. The amyloid-$ß_{(1-42)}$ is associated with AD due to have the most fibrillogenic sequence, having the ability of aggregating in a ß-sheet conformation. However, there are other hypotheses that explain the molecular mechanism of AD, such as the cholinergic hypothesis.

### Amyloid cascade hypothesis

The amyloid cascade hypothesis was formulated more than 20 years ago, and states that the amyloid-ß fibril deposited in amyloid plaques initiates the formation of neurofibrillary tangle formation and several toxic events, leading to neuronal dysfunction, the main pathological effect of AD [60]. However, nowadays it is believed that amyloid-ß oligomers, including protofibrils and prefibrillar aggregates, are the major toxic species in AD [61].

The APP is an integral transmembrane protein consisting in a single membrane-spanning domain, a large extracellular glycosylated N-terminus and a shorter cytoplasmic C-terminus, which is expressed in several tissues, however its concentration is higher in the synapses of neurons [62]. APP can be processed by two main pathways: non-amyloidogenic or amyloidogenic (Figure 2.4). The APP is normally cleaved by α-secretase on the non-

amyloidogenic pathway and processed by ß- and γ-secretases on the amyloidogenic pathway. This results in an imbalance between production and clearance of amyloid-ß peptide. Then, amyloid-ß spontaneously aggregate into soluble oligomers, fibrils and are eventually deposited in neurotoxic amyloid plaques. The formation of these toxic aggregates induce oxidative damage, promote tau hyperphosphorylation, results in toxic effects on synapses and mitochondria, and consequently causes the neuronal loss characteristic of AD [46, 63].

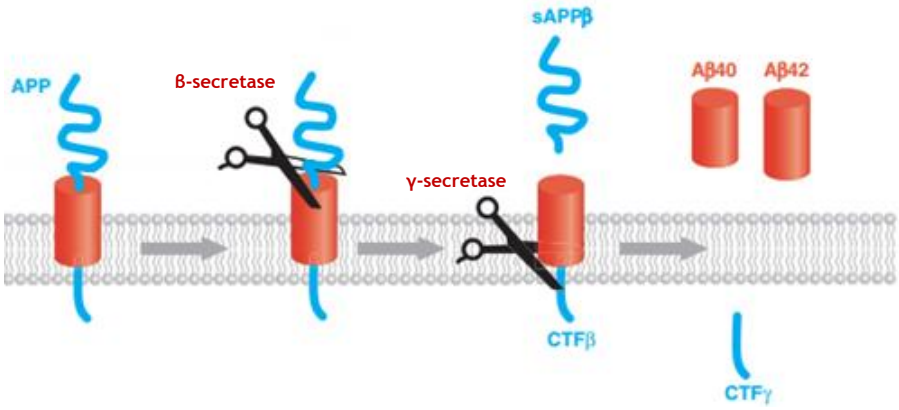


**Figure 2.4** - Production of amyloid-ß peptides. The APPP is cleaved by the ß-secretase resulting on a secreted fragment if APP (sAPPß) and a C-terminal fragment of APP (CTFß). This last one is then cleaved by γ-secretase giving origin to a C-terminal fragment (CTFγ) and amyloid-ß of various lengths (Aß40 and Aß42). The cleavage by α-secretase is not shown, however it cleaves the amyloid- ß domain resulting in the production of amyloid-ß. Image from [64].

### Cholinergic hypothesis

The cholinergic hypothesis defends that a dysfunctional cholinergic system is enough to result in memory deficit, a classical symptom of AD [65]. Moreover, AD patient's brains exhibit degeneration of cholinergic neurons of the basal forebrain and a decline in cholinergic markers (choline acetyltransferase and acetyl cholinesterase) [66]. This hypothesis cannot explain the overall neuropathological features of AD, however it can elucidate an important part of AD's cause.

### Aggregation process of amyloid-ß

Amyloid-ß aggregates in a nucleation-dependent mechanism where partially folded forms of the peptide associate to each other, forming a stable nucleus. Other partially folded intermediates attach to this nucleus, and the aggregated peptide starts to form protofibrils. This chain process continues until the formation of highly structured and insoluble amyloid fibrils occurs. Mainly, the peptide' transition process into fibrils consists of three phases: lag phase, elongation phase and plateau phase. The first one, the lag phase, consists in the unfolding of amyloid-ß and in the formation of oligomers that include species with ß-sheet structures which act as nucleus for the formation of mature fibrils. On the elongation phase, the fibril growths through the addition of monomers or oligomers to the nucleus. Finally, on the plateau phase, the maximum fibril growth is achieved [67, 68].

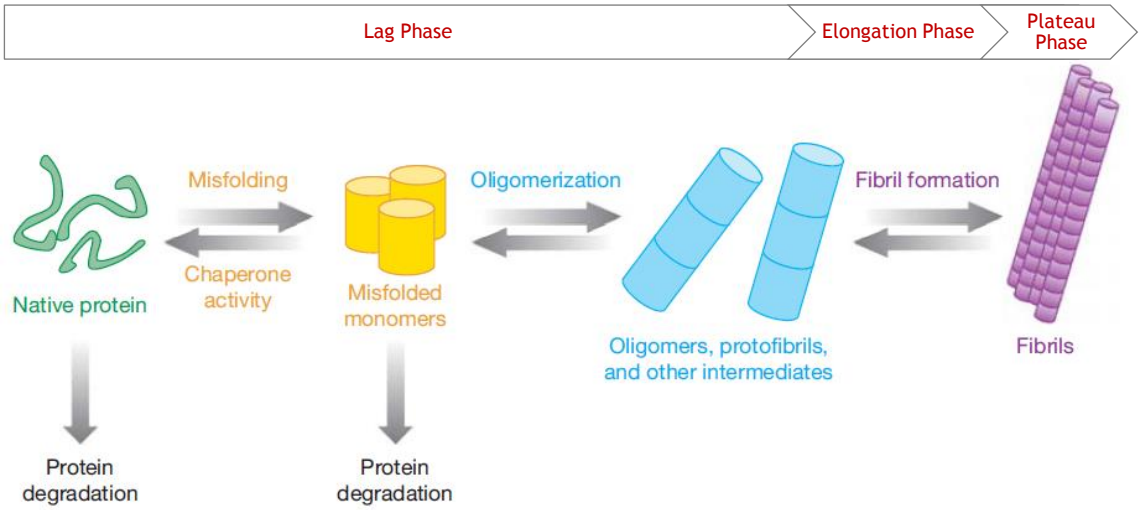


**Figure 2.5** – Process of protein misfolding and fibrillization. The three phases of the transition process are also represented. Image from [64].

## 2.3.2 - Alzheimer's disease-related mutations

There are three genes associates with early onset familial AD, as stated before: amyloid precursor protein (APP), presenilin 1, and presenilin 2. Studies have found several causative mutations of AD in the DNA of subjects who inherited AD, all of them were localized closely to the cleavage sites of β- or γ-secretases and lead to the production of amyloid-$β_{(1-42)}$ or to a change in the aggregation properties of amyloid-β [69, 70]. Mutations in presenilin 1 gene are responsible for the majority of the reported cases of familial AD (FAD), while presenilin 2 gene mutations are relatively rare [69].

## 2.3.3 - Current therapy

Currently, no therapies have been clinically proven to effectively prevent the progression of AD yet, and the actual treatments do not affect the progression of the disease but only attenuate the symptoms of the disease, such as memory and cognitive function. The current therapies are based on cholinergic agents, namely inhibitors of acetylcholinesterase, due to the loss of cholinergic neurons [71]. These agents increase the acetylcholine' levels to prevent the degradation of neurons, however with time the therapy becomes ineffective and the progressive loss of cholinergic neurons continues [49]. Furthermore, a vast majority of other potential AD targets are nearly unaffected by this treatment. The first drug based on this therapy was tacrine (Cognex®), but since it presented hepatotoxic effects, other drugs were developed, such as donepezil (Aricept®), rivastigme (Exelon®) and galantamine (Razadyne®, Reminyl®) [72].

Another therapeutic strategy includes the use of memantine, an N-methyl D-aspartate (NMDA) receptor antagonist. This drug acts by antagonizing glutamate at the NMDA receptor, improving the signal transmission, thus protecting against toxic damage in cholinergic

neurons. This was the first drug to be approved by FDA for treatment in later stages of the disease [50].

Nevertheless, probably the best approach to overcome AD, it to reduce amyloid-β levels in the brain. Thus, several therapeutic strategies have been developed, and they aim to reduce or modulate amyloid-β production, including secretase inhibition and increase of amyloid-β clearance with amyloid vaccines, or to block the aggregation of amyloid-β with different agents, such as antibodies, breaker peptides, or small organic and natural molecules that selective bind and inhibit amyloid-β aggregation, consequently the inhibition of fibril formation is achieved [56, 73]. However, none of them have demonstrated an overall efficiency in stopping the disease progression or reverting the disease state and most of small molecules studied are weekly potent and poorly bioavailable, particularly to the brain.

## 2.3 - The blood brain barrier

Brain drug delivery is still a challenge for the treatment of neurodegenerative diseases. The presence of the blood-brain barrier (BBB) prevents the delivery of most therapeutic agents, thus impeding an effective therapy.

The BBB is an organized interface between peripheral circulation and the central nervous system (CNS) that is capable of responding to local changes and requirements and has a dual function as a barrier and a carrier. It protects the microenvironment of the CNS of fluctuation in the blood composition by blocking the transport of potentially toxic or harmful substances from the blood circulation to the brain, but it allows the crossing of energy substrates and nutrients by specific transport systems. Thus, this interface maintains the CNS homeostasis through the regulation of the ion balance and metabolites influx/efflux [74, 75].

The BBB is present in all brain regions expect in the regions that regulate autonomic nervous system and endocrine glands of the body [76].

### 2.4.1 - Structure and composition

The BBB is composed by different cell types such as endothelial cells, perycites, astrocytes and microglial cells [77]. It consists of two membranes, the luminal and abluminal membranes of the capillary endothelium, which are separated by the endothelial cytoplasm (~200 nm) [78].

Thigh junctions are present within the brain capillary endothelium, connecting adjacent endothelial cells, physically restricting the paracellular diffusion of ions and other polar solutes between endothelial cells [74]. Thus, limiting the passive diffusion to the brain of small lipophilic compounds of molecular weights bellow to 400 Da. Furthermore, the selective influx transport of hydrophilic compounds is permitted by transport proteins [4, 7].

The basal lamina is composed of type IV collagen, fibronectin, heparine sulfate and laminine. It functions as a charge and molecular weight barrier and interacts in complex ways with intergins to regulate permeability and cellular transport across the BBB. Pericytes are macrophage-like cells with smooth muscle properties that are embedded in the basal lamina around the blood vessels. They regulate permeability by release of vasoactive substances. As they decrease with age, there is an increase in the BBB permeability [79].

## 2.4.2 - Transport mechanisms

The transportation of molecules across the BBB can occur through different influx pathways. The transport mechanism by which a molecule is allowed to cross the BBB is dependent of its physicochemical properties.

**Lipid-mediated free diffusion**

A wide range of lipid-soluble molecules are capable of diffusion through the BBB, entering into the brain passively. This capability is correlated with the lipid solubility of the molecule. Base compounds (with a positive charge) are able to cross the BBB due to the interaction with negatively charged glycocalyx and phospholipid head groups of the membrane. Also, blood gases like oxygen and carbon dioxide diffuse across the BBB dependent of the concentration gradient [74]. Thus, the restriction of entry into the CNS is dependent on the molecule structural physicochemical properties, such as size (< 400-500 Da), charge, hydrogen bounding potential (< 8-10 hydrogen bonds with water) and lipophilicity [77, 78].

**Carrier- or receptor-mediated transport**

Since the majority of the polar molecules cannot diffuse through cell membranes, cells express a large number of solute carriers, like choline and amino acid transporters, in the cell membrane. The orientation of these transporters results in preferential transport of substrates into or across the cell. Thus, the direction of the transport may be from blood circulation to the CNS or vice-versa [74].
Essential large molecules for the brain homeostasis, such as amino acids, hexoses, neuropeptides and proteins, cross the BBB through endocytotic mechanisms involving either receptor-mediated transcytosis (RMT) or adsorptive-mediated trancytosis (AMT). RMT requires the binding of macromolecules to specific receptor on the cell, inducing endocytosis and subsequent transcytosis. On the other hand, AMT depends on the ligand electrostatic interaction with the surface charge of the endothelial cells for triggering endocytosis followed by transcytosis [74]. The main targets for RMT are transferrin receptor (also highly expressed in the liver, heart and other cells), insulin receptor (also highly expressed in adipose tissue, liver and muscle cells) and low-density lipoprotein (also highly expressed in the liver) [80].

**ATP-binding cassette transporters**

The main role of the ATP-binding cassette transporters (ABC transporters), such as p-glycoprotein (P-gp), is to function as an active flux pump that consumes ATP and transports potentially neurotoxic endogenous or xenobiotic molecules out of the CNS. Thus, these receptors have a vital neuroprotective and detoxifying function [74].

### 2.4.3 - A barrier to conventional therapy – methods to increase the transport

The majority of the therapeutic drugs are not capable to reach the CNS in a therapeutically relevant concentration due to the relative impermeability of the BBB. Therefore, BBB is the major impediment in the treatment of CNS disorders [81]. Nowadays, most of the new drug candidates to treatment of CNS disorders are large molecules that have poor pharmacokinetics and cannot cross the BBB. Additionally, approximately 98% of all small molecules are not transported across the BBB [78].

Briefly, the restrict access to the brain is due to several characteristics of BBB, the existence of tight junctions that block the passage through the intercellular gap, the reduced rate of pinocytosis on the luminal side, the nonexistence of fenestrations, the enzymatic barrier (considered a second line of protection) and, finally, due to the efflux transport system [80].

In order to overcome the limited access of therapeutic drugs to the brain, there are several methods to increase the transport from blood into the CNS [40, 82]. The most accepted is the physiological approach which takes advance of the receptor transcytosis capacity. In this non-invasive approach, drugs are modified to be recognizable by the nutrient transport system of BBB or are conjugated with ligands that recognize expressed receptors at the BBB. However, it can have some disadvantages, for instance the possible non-specific drug-receptor interactions in peripheral organs. Meaning that an high concentration of the drug with these target molecules can bound in other organs before they can reach the BBB [80]. Also, drugs can be modified to reduce the relative number of polar groups and increase the cross of it through the BBB. But, this can lead to loss of desired activity of modified drugs and extrusion of the drug outside with efflux pump due to increased drug lipophilicity [7]. Moreover, the inhibition of the efflux transporters can improve the treatment efficacy, but it can also result in intolerable adverse side effects after efflux inhibition [77].

Other method is the invasive approach, which include several expensive technology that involve a high risk complications, such as intracerebroventricular infusion, convection enhanced delivery, disruption of BBB and polymeric or microchip systems. This method breaches the BBB mechanically in order to deliver drug to the brain [7, 77].

However, there is a promising way to cross the BBB and deliver drugs to targets within the CNS through the use of nanoparticles. It has already been demonstrated that the nanoparticles with their surface modified are capable to cross the BBB into the brain after intravenous administration via receptor-mediated pathways.

## 2.4 - Nanoparticles as drug delivery systems for neurodegenerative disease' therapy

Nanoparticles are a class of drug delivery system which are able to target a certain part of the body for delivery of the therapeutic drug. The nanoparticle size vary in a range of 10 to 1000 nm and can be constructed from various materials and carry an extensive variety of active compounds, such as chemotherapeutics, contrast agents, proteins and nucleic acids [7].

Nanoparticles allow the transportation of therapeutic drugs for PD and AD across the BBB, that otherwise was not possible, by masking the limiting physicochemical properties of these molecules through their encapsulation. Thus, it does not require the modification of the drug molecule, because the ability to cross the BBB is only dependent of nanoparticle's properties [77]. Furthermore, the use of nanoparticles allows a reduction of the required doses by improving of the pharmacological and therapeutic properties of the drug, as well as a decrease peripheral and/or systemic toxicity [4, 7, 40].

This system can be administered directly into the brain or they can be systemic delivery with a target action in the central nervous system [40]. The delivery across the BBB is mostly achieved through receptor-mediated endocytosis of the nanoparticles by brain capillary endothelial cells followed by transcytosis. The receptors available for targeting are, for example, lipoprotein, scavenger transferrin and insulin receptors [77].

Since the ability to cross the BBB is not dependent of the chemical structure of the drug encapsulated, but of the physicochemical and biomimetic features of the nanoparticle, they must have several properties that make them suitable to be used for drug delivery across the BBB. These properties include nontoxicity, biodegradability, biocompatibility, non-immunogenicity (unless it is targeting the monocytes/macrophages), stability in blood (no aggregation and dissociation), capacity of interacting with receptors present at the BBB, controllable drug releasing profiles, and ability to carry small molecules, proteins, peptides or nucleic acids [83, 84]. The nanoparticle must have a controlled size in order to have its properties uniform and consistent, but also to have to control of its biological fate [83]. Moreover, the nanoparticle size have influence on the endocytotic uptake mechanism. Commonly, nanoparticles with a size below to 200 nm are up taken by clathrin-mediated endocytosis, whereas nanoparticles with a size up to 500 nm are uptaken caveolae-mediated endocytosis [77]. However, they can also enter in the cells through a passive mechanism, by direct plasma membrane penetration [80].

The nanoparticle surface charge and hydrophobicity have influence on the nanoparticle uptake and/or the rate of transyctosis due to their influence on the pattern of proteins adsorbed from plasma. It is known that hydrophobic surfaces are rapidly opsonized followed by recognition by the reticuloendothelial system (RES), and higher internalization rates are usually associated with positively charged nanoparticles due to the negatively charged composition of the biological membranes. However, negatively charged nanoparticles can achieve efficient uptake rates after the adsorption or covalently coupling of targeting ligands. Still, the nanoparticle surface is not the only one to have influence on the successful brain delivery, but all the materials used in the nanoparticle formulation may influence their ability to deliver drugs across the BBB [77]. Thus, when designing the nanoparticle it is essential to give attention the surface materials chosen, but also to the core materials.

In Table 2.3 are resumed some of the studies of encapsulation of therapeutic drugs in nanoparticles for targeted brain delivery, mainly for the treatment of PD and AD. The majority is trying to encapsulate drugs that are already used in the treatment, however some recent studies are using antioxidants and growth factors as new rising therapies that can prevent the progress of the disease or even reverse it.

**Table 2.3** – Studies published using drug brain delivery systems, mainly for the treatment of PD and AD. The studies are divided by type of therapeutic drug used, material, targeting ligand and administration route (systemic or local). GDNF: Glial cell line-derived neurotrophic factor, BDNF: Brain-derived neurotrophic factor, VEGF: Vascular endothelial growth factor.

| Therapeutic Drug | Material | Targeting Ligand | Administration Route | Model | Ref. |
|---|---|---|---|---|---|
| **Dopamine** | Chitosan nanoparticle | - | Intraperitoneal | *In vitro* | [85] |
| | Molecular carrier | Amino acid derivates | Intraperitoneal | - | [86] |
| | Alginate scaffold embedding stable D-loaded celulose acetate phthalate nanoparticle | - | Local | Healthy Sprague-Dawley rats | [87] |
| | Liposome | - | - | *In vitro* | [88] |
| **Succinyl Dopamine** | Quantum rods/amphiphilic polymer/PEG | Galactose | Local | *In vitro* | [89] |
| **GDNF** | PLGA nanoparticle | - | Local | 6-OHAD rat model | [90] |
| | Lactoferrin-modified nanoparticle | - | - | | [44] |
| | PAMAM/PEG nanoparticle | Lactoferrin | Intravenous | Rotenone rat model | [91] |
| **GDNF fused with collagen binding peptide** | PLGA/Collagen nanoparticle | - | Local | *In vitro* | [92] |
| **GDNF and BDNF** | PLGA microparticle within a PEG-based hydrogel | - | Local | *In vitro* | [93] |
| **GDNF and VEGF** | PLGA nanoparticle | - | Local | 6-OHAD rat model | [94] |
| **Neurotrophin-3 and MIAMI stem cells** | PLGA microparticle with a biomimetic surface | - | Local | 6-OHAD rat model | [95] |
| **Plasmic GDNF** | DNA compacted by polycations to form colloidally stable NP | - | Local | 6-OHAD rat model | [96] |
| **Sialic acid** | Poly(N(2-hydroxypropyl) methacrylamide) | - | Local | 6-OHAD rat model | [97] |
| **Levodopa-α-lipoic acid** | PLGA microparticle | - | Subcutaneous | - | [98] |
| **Levodopa methyl ester and benserazide (decarboxylase inhibitor)** | PLGA nanoparticle | - | Subcutaneous | 6-OHAD rat model | [99] |
| | Polymeric nanoparticle | - | - | LDA-stimulated dyskinetic rat model | [100] |
| **Levodopa** | Chitosan nanoparticle thermoreversible to gel | - | Intranasal | - | [101] |
| | Liposome-PEG | Chlorotoxin | - | *In vitro* | [102] |
| **Rotigotine (agonist)** | PLGA microparticle | - | Intramuscular | 6-OHAD rat model | [103] |
| **Apomorphine (agonist)** | PLGA microparticle | - | - | - | [104] |
| | Tripalmitin hydrogenated soybean phosphatidylcholine solid lipid nanoparticle | - | Oral | 6-OHAD rat model | [105] |
| **Ropinirole (agonist)** | Nanoemulsion | - | Transdermal | 6-OHAD rat model | [106] |
| **Bromocriptine (agonist and antioxidant)** | Chitosan nanoparticle | - | Intranasal | Haloperidol rat model | [107] |
| | Solid lipid nanoparticle | - | - | - | [108] |
| **Tempol (antioxidant)** | PLGA microparticle | Ab OX-26 Transferrin receptor | - | *In vitro* | [109] |

| | | | | | |
|---|---|---|---|---|---|
| **Rasagiline (MAO B inhibitor)** | PLGA nanoparticle | - | Intraperitoneal | Rotenone rat model | [110] |
| **Urocortin** | PEG-PLGA nanoparticle | Lactoferrin | Intravenous | 6-OHAD rat model | [111] |
| | Lactoferrin-modifed nanoparticle | - | - | - | [44] |
| | PEG-PLGA nanoparticle | Odorranalectin | Intranasal | 6-OHAD rat model | [112] |
| **Nerve growth factor** | Poly butylcyanocrylate nanoparticle | Polysorbate-80 | Intravenous | MPTP rat model | [113] |
| **Chelating ligands (CuAC, EDTA, histidine and ZnAc)** | Nanoliposome | - | - | *In vitro* | [114] |
| **Curcumine** | PLGA nanoparticles | Tet-1 protein | - | - | [115] |
| **Bromocriptine** | Tristearin/tricaprin nanostructures-solid lipid nanoparticle | - | - | 6-hydroxydopamine hemilesioned rat model | [116] |
| **Phosphatidic acid** | Nanoliposome | Apoliprotein E | - | hCMEC/D3 cells | [117] |

## 2.4.1 - Solid lipid nanoparticles

Solid lipid nanoparticles (SLN) are a stable lipid-based nanoparticles composed by a solid hydrophobic lipid core where the therapeutic drug can be dissolved or dispersed (Figure 2.6). However, SLN are also feasible of incorporating hydrophilic drugs on their surface. These nanoparticles are made of an oil/water emulsion with lipids that are solid at room temperature and body temperature [118]. Their size is between 40 to 200 nm providing them the ability to cross tight endothelial cells of the BBB, escape from the reticulo-endothelial system (RES), and thus bypass liver and spleen filtration. In addition, the synthesis of these nanoparticles is cost effective, have excellent reproducibility and avoid the use of organic solvents [36].

Besides having all the requirements described on the last section, SLN formulations are stable for approximately 3 years and the controlled drug release can be made to last several weeks. Triglycerides, fatty acids and waxes are examples of lipid used in the synthesis of SLN [84, 108].

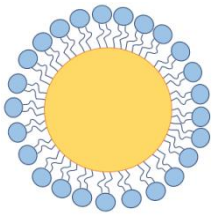

**Figure 2.6** - Schematic representation of a solid lipid nanoparticle.

## 2.4.2 - Functionalization

After intravenous injection, the nanoparticles are rapidly opsonized and cleared from the blood stream by the macrophages of the RES which are mainly localized in the liver and spleen [77, 82]. However, the blood circulation time of the nanoparticle can be prolonged by modification of the nanoparticle surface with surfactants or by covalent attachment of hydrophilic surfactants, such as polysorbates or polyethylene glycol (PEG) chains to the core polymer. Thus, the mass of drug delivered to the brain is proportional to the BBB permeability coefficient and the area under curve plasma concentration versus time [77].

Besides increasing the blood circulation time, PEG grants steric stabilization of the nanoparticle surface, allowing the attachment of ligands (e.g. antibodies, proteins or aptamers) capable of binding to BBB nutrient transport systems or internalizing receptors [84]. It is known that the ligands attached to the nanoparticle may increase the elimination rate by the RES, however the coverage of the nanoparticle with PEG reduces this effect [83].

The functionalization of the nanoparticle by covalent conjugation of various ligands can be used to target specific tissues, like the brain, enhancing the bioavailability of a drug, that otherwise was not able to cross the BBB, in that specific *locus*. Moreover, the functionalization of the nanoparticle surface can improve the crossing through the BBB by allowing an electrostatic interaction with the luminal surface of the BBB. This can be achieved by conferring a positive charge to the nanoparticles surface through functionalization with positively charges molecules. Thus, nanoparticles can be multifunctional and have several properties like drug delivery, targeting and diagnosing capabilities [7].

The selection of the ligands is extremely critical since the receptor should be preferentially expressed at the BBB, but ideally it should be brain specific in order to reduce potential side-effects and increasing transport efficiency [83]. Also, the natural saturation of the receptor must be considered to avoid competition with the natural ligand [84]. Some possibilities of molecular and cellular targets that can be focus for drug delivery therapy for PD are α-synuclein protein, leucine-rich repeat serine/threonine protein kinase 2 and the parkin protein, and for AD could be for example molecular targets that can act on α-, β-, and γ-synuclein peptides [40].

If a fluorescent probe is conjugated with the nanoparticle targeted to a PD or an AD biomarker it is possible to diagnose and follow the progress of these diseases. The copulation of this property with the simultaneous ability of delivering drugs is denominated theranostic [7].

Figure 2.7 is a representation of a nanoparticle where the drug is both encapsulated in the core and conjugated at the surface. Here are represented the vast kind of molecules that can be functionalized at the nanoparticle surface with the objective of targeting the brain (antibody, peptide, aptamers and cationic molecules), avoid the RES (PEG) and imaging purposes (fluorescent probe) [84].

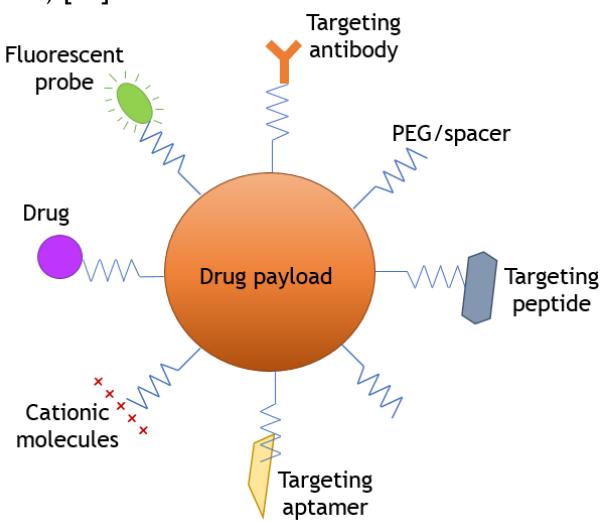


**Figure 2.7** - Representation of a multifunctionalized nanoparticle with drugs (encapsulated in the core or conjugated at the surface), brain targeting molecules (antibodies, peptides, aptamers and cationic molecules), PEG and a fluorescent probe. Adapted from [84].

### 2.6.1 - Monoclonal antibodies

The transferrin receptor (TfR) is expressed at a high level in the brain capillary endothelium, thus the targeted delivery of therapeutic compounds to it allows a greater therapeutic outcome [109]. However, transferrin is not an ideal TfR-targeting ligand due to the competition with the transferrin present in the bloodstream, leading to the saturation of these receptors [119, 120]. In order to overcome this problem, antibodies against the transferrin were developed, such as the OX-26 antibody [121].

## 2.5 - Resveratrol as a potential therapy for neurologic diseases

Resveratrol (3,5,4'-trihydroxystilbene) is a natural polyphenolic flavonoid, which can be found in nature as both cis and trans isomers, being the last considered to be the most abundant and biologic active. Several effects have been related with the intake of resveratrol, such as anti-carcinogenic, anti-inflammatory, anti-obesity and heart/brain protective effects (modulation of nitric oxide biosynthesis and activity) [6]. The neuroprotective effects of resveratrol in neurological disease, such as AD and PD, is related to the protection of neurons against oxidative damage and toxicity (due to ROS production), and to the prevention of apoptotic neuronal death [6, 51].

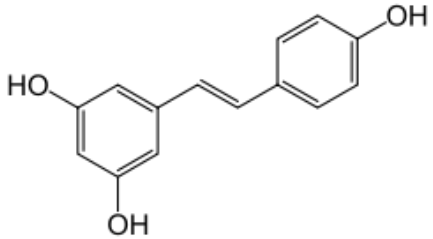


**Figure 2.8** – Chemical structure of resveratrol.

However, after intravenous injection, resveratrol is rapidly absorbed, metabolized into both glucuronic acid and sulfate conjugations of the phenolic groups in the liver and intestinal epithelial cells (within less than 2 hours), which are eliminated posteriorly [49].Thus, resveratrol has low bioavailability, limiting its biological and pharmacological benefits. It also has poor water solubility and is chemical instable, being degraded by isomerization when expose to elevated temperatures, pH changes, UV light or certain types of enzymes [6].

Furthermore, resveratrol has the ability of mimicking the healthy benefits of calorie restriction, also called dietary restriction, which is known that it leads to the stimulation of stress proteins and to the increase of the organism's defense mechanisms [51]. Consequentially, this effect enhances the longevity of the organisms, but also protects the organism from stress. However, long-term effects of this treatment on neurodegenerative diseases were not studied yet, and the short-term adverse effects includes infertility, menstrual irregularities, hypertension, loss of libido, loss of strength and stamina, slower wound healing, depression and even irritability [49].

Resveratrol can be found in the seeds and skins of grapes, red wine, mulberries, peanuts, rhubarb and in several other plants [51]. It's concentration in the skin and seeds of grapes is approximately 50-100 ug per gram, corresponding to 5-10% of their biomass, nonetheless it varies considerably on different grape vine cultivars [6, 51]. This fact is associated with the *French Paradox*, which is refers to the beneficial effects of a moderate consumption of red

wine. Besides resveratrol, both red wine and purple grapes (specially the skin and seeds) contain several flavonoids, such as quercetins, catechins, gallocatechins, procyanidins, and prodelphidins [49].

# Chapter 3

# Materials and methods

## 3.1 - Materials

For the nanoparticles synthesis, trans-resveratrol (more than 99% pure) and polysorbate 80 (Tween® 80) were purchased from Sigma-Aldrich (St Louis, MO, USA), the solid lipid cetylpalmitate was provided by Gattefossé (Nanterre, France). The grape's skin and seed extracts were provided by BioPolyphenols (DoisPortos, Portugal) and Monteloeder (Elche, Spain), respectively.

For the nanoparticle functionalization, 1,2-Distearoyld-sn-Glycero-3-Phosphoethanolamine -N-maleimide(polyethylene Glycol)2000 was purchased from Avanti Polar Lipids (Alabaster, Alabama, USA), and the monoclonal antibodies for transferrin BBB receptors, OX-26 mAb, were purchased from AbD Serotec (Kidlington, UK). For the ELISA assay the human transferrin receptor peptide was bought from Abcam® (Cambridge, UK) and the secondary antibody, Goat anti-mouse IgG (H+L), was purchased from Thermo Fisher Scientific (Waltham, MA USA).

For the grids preparation for morphological analysis on TEM, uranyl acetate was purchased from Electron Microscopy Sciences (Hatfield, PA, USA).

The α-synuclein human and the ß-amyloid (1-42) human, for the kinetics studies were purchased from Sigma-Aldrich (St Louis, MO, USA) and GenScript (Piscataway, NJ, USA), respectively. Moreover, the Thioflavin T was provided by Sigma-Aldrich (St Louis, MO, USA).

The water used in all experiments during this project was purified water by Ultra-pure water system (Milli-Q RG), and was obtained from a reverse osmosis process.

## 3.2 - Methods

### 3.2.1 - Solid lipid nanoparticles preparation

The method used for the nanoparticle synthesis is a compromise between the high shear homogenization method and the ultrasonication method, and it is represented in Figure 3.1. Hence, it is possible to produce particles with a micrometer size by the first method, and then, reduce their size to the nanometer size range by the second method.

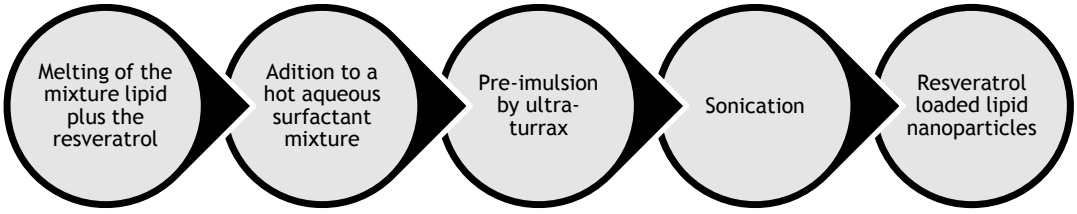


**Figure 3.1 -** Scheme of the preparation method of the solid lipid nanoparticles.

The lipid phase, containing DSPE-PEG(2000)maleimide, the cetylpalmitate (solid lipid), the stabilizer polysorbate 80 and the drug to be encapsulated (0, 2, 5, 10 or 15 mg) was melted at 70ºC, which is above the lipid's melting point. The melted lipid was then dispersed in ultrapure water, at the same temperature, by high-speed stirring in an Ultra-Turrax T25 (Janke and Kunkel IKA-Labortechnik, Staufen, Germany) followed by sonication (70% amplitude) using a Sonics and Materials Vibra-Cell™ CV18 (Newton, CT, USA). The nanoemulsion was let cooling at room temperature to allow the crystallization of the lipid and consequent formation of the solid lipid nanoparticles.

**Table 3.1** - Chemical structure of the lipids used for the synthesis of the solid lipid nanoparticles.

| Name | Structure |
|---|---|
| **Cetylpalmitate** | 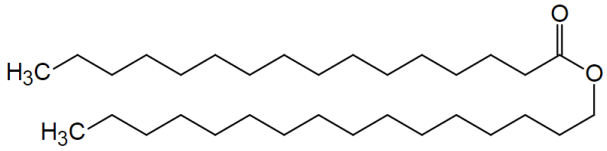 |
| **Polysorbate 80** | 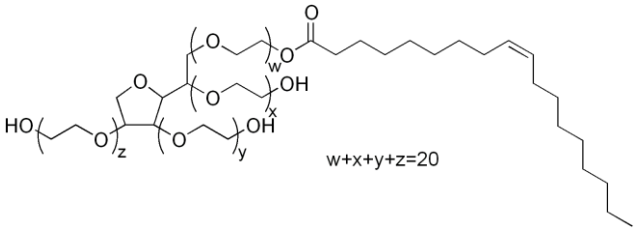 |
| **DSPE-PEG(2000) Maleimide:** 1,2-distearoyl-sn-glycero-3-phosphoethanolamine-N-(maleimide(polyethylene glycol)-2000) | 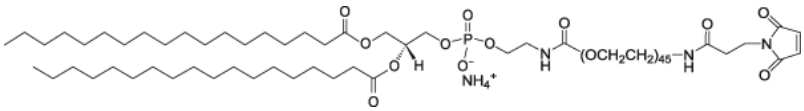 |

The parameters of both techniques were previously optimized to establish the best conditions for the production of a stable formulation with an average size of less than 200 nm. The final parameters chosen were a high shear homogenization of 2 minutes at 12000 rpm, and a 15 minutes sonication at intensity of 70%.

Three different compounds were encapsulated on the lipid nanoparticles: pure resveratrol, grape's seeds and skin (with and without centrifugation).

The formulations were storage for at least 1 month protected from light, at room temperature, and they were characterized periodically in order to access the stability of the nanoparticles. Moreover, the effect of different drug/lipid ratio was assessed.

### 3.2.2 - Conjugation of the antibodies

Covalent coupling methods for attaching the antibodies at the PEG terminus by using functionalized PEG with a chemically reactive end-group were applied. For the maleimide-mAb conjugation, the target was activated by a twenty times molar excess of Traut's reagent (2-iminothiolane hydrochloride, MW 137.73, Sigma-Aldrich). Moreover, a drop of EDTA (ethylenediaminetetraacetic acid, MW 292.40, Sigma-Aldrich) 0.28 M was added to prevent metal catalysed oxidation of sulfhydryl groups. The unreacted EDTA/2-iminothiolane complexes were removed through application of a size exclusion chromatography using a Sephadex column PD-Minitrap G25 (GE Healthcare). After the conjugation with the antibodies, samples were incubated at room temperature for 1 hour and then at 4 ºC overnight. The antibodies were added to the solid lipid nanoparticles at a molar ratio of 1:1 between antibodies and functionalized PEG.

The affinity of the conjugated solid lipid nanoparticles for transferrin (TfR) was analysed by ELISA. For this, the surface of a 96-well plate (flat-bottom Nunc MaxiSorp®) was coated with TfR during 1 hour at 37 ºC. The plate was then blocked with BSA (bovine serum albumin, ~66 kDa) and incubated for another hour at 37 ºC, followed of addition of the nanoparticles to each well. After incubation and subsequent washing, the secondary antibody, which was conjugated with peroxidase, was let react during 45 minutes at room temperature. The reveal solution was composed by citric acid (MW 210.14, Sigma-Aldrich), ABTS (2,2′-azino-bis(3-ethylbenzothiazoline-6-sulfonic acid) diammonium salt, MW 548.68, Sigma Aldrich) and $H_2O_2$ (hydrogen peroxide solution, MW 34.02, Sigma Aldrich), and the absorbance spectrum of each well was read at 405 nm using a Biotek Synergy 2 spectrometer. Furthermore, nanoparticles without being conjugated were used as a negative control.

### 3.2.3 - Nanoparticles size

The nanoparticles size was measured by dynamic light scattering (DLS). DLS allows the determination of particle size and size distribution in dispersions (polydispersity index, PI). The results are based on fluctuations of the light scattered intensity as a function of time, which are directly related to the Brownian motion of the solute and can be related with their diffusion coefficient [122]. Therefore, the SLN size of monodisperse nanoparticles can be calculated using the Stokes-Einstein equation [123]:

$$R_H = \frac{kT}{6\pi\eta D} \tag{3.1}$$

where, $R_H$ is the hydrodynamic radius, k is the Boltzman constant, $T$ is the temperature, $\eta$ is the viscosity of the solvent and $D$ is the diffusion coefficient of the nanoparticles.

Samples were diluted (1:200) in ultrapure water to achieve a suitable scattering intensity, which is translated into an average count rate between 100 and 500 kcps. The formulations were analysed at 25ºC and both size and PI were calculated through the average of 10 runs, in triplicate.

### 3.2.4 - Zeta potential

Zeta potential of the lipid nanoparticles was measured by electrophoretic light scattering (ELS). It is known that nanoparticles in suspension attract ions to their surface, forming an electrical double layer at the nanoparticle surface (an inner layer where ions are strongly adsorbed to the surface, and an outer layer where ions diffuse more freely). Zeta potential is defined as the electric potential that exists in the diffuse boundary of the nanoparticle (boundary of the outer layer with the bulk solution). It can be calculated using Henry's Law [124]:

$$U_E = \frac{2\varepsilon z f(ka)}{3\eta} \tag{3.2}$$

where, $U_E$ is the electrophoretic mobility, $z$ is the zeta potential, $f(ka)$ is the Henry's function and η is the viscosity coefficient. Zeta potential is an indicator of the stability of the nanoparticle suspension [125].

Samples were diluted (1:200) in ultrapure water, transferred to folded capillary cells from Malvern (Worcestershire, UK) and their zeta potential was obtained by the average of 3 measurements (each one with 12 runs) using a ZetaSizer Nano ZS (Malvern Instruments, Worcestershire, UK).

### 3.2.5 - Morphologic analysis

The nanoparticle morphology was characterized by transmission electron microscopy (TEM). In this technique, an electron beam hits the sample and part of it is transmitted through the sample, reaching to a phosphor screen where the image is formed. The differences on the image contrast are dependent of the amount of electrons that did not interacted with the sample and were able to pass through it. Therefore, darker regions are due to the few electrons that were transmitted as a result of higher thickness or density of the sample, and brighter regions results of a higher electron transmission [122].

Nanoparticles samples were prepared on 400 mesh Formvar/Carbon copper grids (Agar Scientific, Essex, UK). For this, 5 µL of each sample was placed on the mesh and let to absorb for five minutes. The negative staining (2% filtered aqueous solution of uranyl acetate) was let react for 45 seconds, the excess was removed and the grid was let drying. The morphological analysis was accessed on a JEOL JEM-1400 TEM at an accelerating voltage 80kV (Tokyo, Japan).

### 3.2.6 - Determination of entrapment efficiency

The entrapment efficiency (EE) of the compounds was determined through the difference between the amount used in the formulation synthesis and the amount that remained free in the aqueous phase, as follows:

$$\%EE = 1 - \frac{Unentrapped\ drug}{Total\ amount\ of\ drug} \times 100 \quad (3.3)$$

Samples of the different formulations were diluted in ultrapure water (1:200), transferred into Amicon® Ultra Centrifugal Filters (Merck Millipore, Billerica, MA, USA), and centrifuged using a Allegra® X-15R Centrifuge (Beckman Coulter, Pasadena, CA, USA) during 25 minutes at 4300 rpm. Afterward, the free drug present in the supernatant was collected and quantified using a V-660 spectrophotometer (Jasco, Easton, MD, USA) at 200-600 nm.

### 3.2.7 - Determination of the yield

The yield was determined by calculating the weight difference of the samples before and after filtration (Equation 3.4). In order to do this, two set of samples, one filtrated and the other non-filtrated, were let dry out and the remaining lipid was weighted. This assay allows knowing an approximation of the quantity of nanoparticles lost with filtration.

$$Yield\ (\%) = \frac{remaining\ lipid\ after\ filtration}{remaining\ lipid\ before\ filtration} \times 100 \quad (3.4)$$

### 3.2.8 - Fluorescence measurements and Thioflavin T binding assay

Interaction of the nanoparticles with α-synuclein and amyloid-β was evaluated through the Thioflavin T (ThT) binding assay. ThT is a common amyloid dye, which binds rapidly to to amyloid fibril structures, have a strong fluorescence emission. Furthermore, the intensity of the fluorescence is proportional to the quantity of amyloid fibrils [126].

A ThT sock solution was prepared in phosphate buffer saline (PBS) or sodium phosphate buffer at the concentration of 0.8mg/mL, and a ThT working solution was prepared by diluting 1mL of the stock solution in 50mL of buffer. Samples containing α-synuclein (final concentration of 20 μM) in sodium phosphate buffer, and samples containing amyloid-β (final concentration of 25 μM) in PBS, were filtered, diluted and added to the ThT working solution immediately after preparation. The samples were placed on a 96-well plate (Nunclon Delta Surface) and the intensity was measured on a Biotek Synergy 2 fluorescence spectrometer (Winooski, USA) after stirring 30 seconds every 15 minutes during 10 days. The temperature was maintained constant at 37ºC.

### 3.2.9 - Statistical analysis

The statistical analysis was performed using SigmaPlot™ software (v 13.0; Systat Software, CA, USA). The measurements were at least three times and data were expressed as mean ± SD. Data were analysed using two-way analysis of variance (two-way ANOVA), followed by Holm-Sides and Tukey tests. A *P* value of 0.05 was considered statistically significant.

# Chapter 4

# Results and discussion

## 4.1 - Physicochemical characterization of solid lipid nanoparticles

Unloaded solid lipid nanoparticles were synthesized by the hot homogenization technique and characterized. The mean size of the unloaded nanoparticles measured by DLS was 142 ± 10 nm. This size corresponds to the required size for brain drug delivery [127].

The PDI of the unloaded SLN was 0.12 ± 0.04 showing that the formulation has a monodisperse population.

The zeta potential of the nanoparticles was -0.08 mV. In this case, the nanoparticles exhibited low electrostatic stabilization, but they still are stable.

In order to choose the more favourable drug concentration for SLN, formulations with different concentrations of grape's extracts (2, 5, 10 and 15 mg) were prepared and characterized according to their entrapment efficiency, average size and zeta potential.

The grape's extracts loaded-nanoparticles mean size is presented in Figure 4.2. All formulations showed a homogeneous size distribution with a mean diameter between 150 nm and 200 nm, except the nanoparticles loaded with centrifuged grape's seeds, which achieve a mean size higher than the required size range. Although there was no statistically difference (P>0.05).

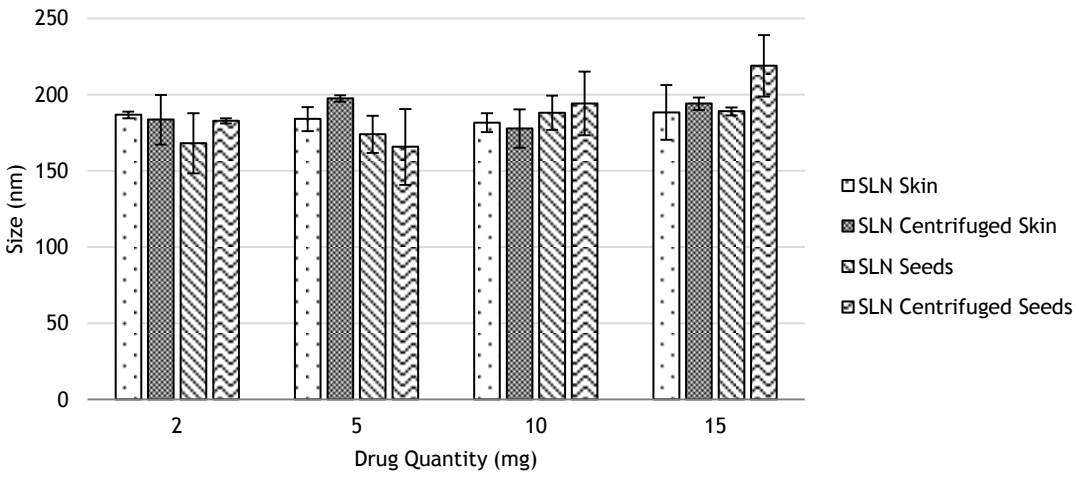


**Figure 4.1 – Mean s**ize of the nanoparticles (skin, centrifuged skin, seeds and centrifuged seeds). All values represent the average and the standard deviation (n=3).

As the unloaded SLN, the zeta potential of the different extracts-loaded nanoparticles was almost neural, meaning that the encapsulation of these compounds did not have impact on the zeta potential (Table 4.1) as no statistically significance differences where observed between any of the formulations ($P > 0.05$).

**Table 4.1 -** Zeta potential of the nanoparticles (skin, centrifuged skin, seeds and centrifuged seeds). All values represent the average (n=2).

| SLN | Quantity of drug (mg) | | | |
|---|---|---|---|---|
| | **2** | **5** | **10** | **15** |
| **Skin** | 0.07 | 0.18 | -0.07 | -0.34 |
| **Centrifuged Skin** | -0.11 | -0.16 | -0.09 | 0.01 |
| **Seeds** | -0.17 | -0.06 | 0.35 | -0.21 |
| **Centrifuged Seeds** | -0.06 | 0.05 | 0.02 | -0.02 |

The encapsulation efficiency of each of these formulations is shown of Figure 4.2. Generally, the percentage of encapsulation was higher than 60%. It is also possible to observe that increasing the extract concentration, the entrapment efficiency decreases as it would be expected. However, these differences on the percentage of drug encapsulated were not significant ($P>0.05$). The main natural resource of resveratrol is the grape, but its concentration present on the extracts is very low (20 mg/kg of dry skin and 6.8 mg/kg of dry seed) [128]. Therefore, calibration curves (Annex A) were made for all the compounds used, since the percentage of resveratrol present in the grape's extracts is too low to be detected by absorbance without being affected by others compounds present in the extracts that also can absorb at the same wavelength [128].

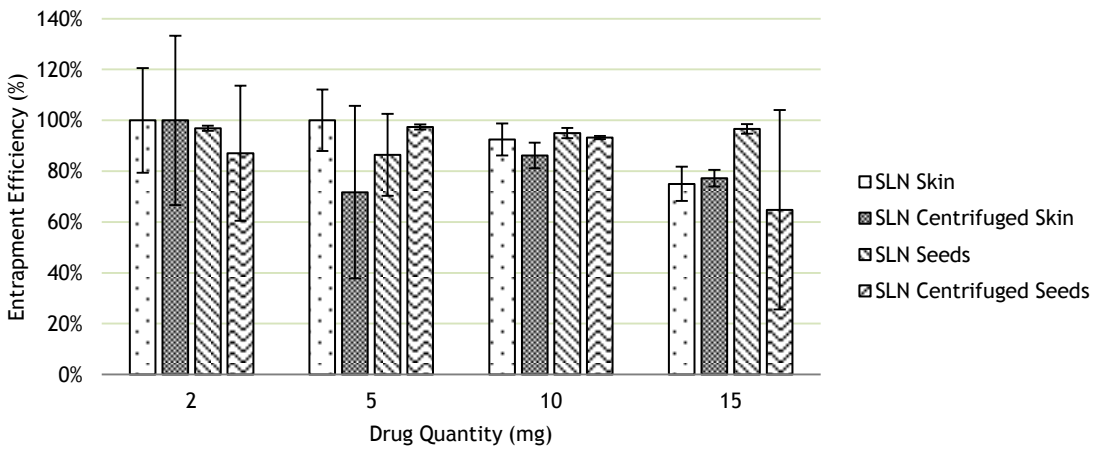


**Figure 4.2** – Entrapment efficiency of the nanoparticles (skin, centrifuged skin, seeds and centrifuged seeds) in percentage of compound encapsulated (calculated through the calibration curve of each drug: Annex A). All values represent the average and the standard deviation (n=2).

Taking the previous results in account, the final drug concentration chosen was 10 mg. The next step was to synthetize resveratrol-loaded nanoparticles and proceed to their characterization and other studies.

In Table 4.2 are presented the average size, polidispersity index, zeta potential and entrapment efficiency of the nanoparticles synthetised with 10 mg of drug and of the unloaded nanoparticles. The formulations appeared white (unloaded and resveratrol), beige (seeds and centrifuged seeds) or pink (skins and centrifuged seeds) and had low viscosity.

All of the formulation showed a homogeneous size distribution, with a a size inferior to 200 nm with the PI inferior to 0.2, indicating that the formulations have a good monodispersity distribition, with low variability and no aggregation.

**Table 4.2** – Characterization of the lipid nanoparticles (10mg of drug). All values represent the average and the standard deviation (n=3).

| SLN 10mg | Size (nm) | Polidispersity Index | Zeta Potential (mV) | Entrapment Efficiency (%) |
|---|---|---|---|---|
| **Unloaded** | 142 ± 10 | 0.12 ± 0.04 | -0.08 | - |
| **Resveratrol** | 176 ± 24 | 0.16 ± 0.10 | 0.17 | 94 ± 9 |
| **Grape's skin** | 182 ± 6 | 0.11 ± 0.04 | -0.07 | 93 ± 6 |
| **Centrifuged grape's skin** | 178 ± 13 | 0.11 ± 0.04 | -0.09 | 86 ± 5 |
| **Grape's seeds** | 188 ± 11 | 0.13 ± 0.04 | 0.34 | 95 ± 2 |
| **Centrifuged grape's seeds** | 194 ± 21 | 0.11 ± 0.04 | 0.02 | 94 ± 6 |

There was no significative differences on the zeta potential of all formulations, also meaning that the encapsulation of the different compounds did not altered the surface charge of the nanoparticles.

The entrapment efficiency of all the formulations synthesized achieved an high percentage value around 90%, suggesting that the lipid nanoparticles are a suitable system for the incorporation of both resveratrol and grape's extracts. This is confirmed by the fact of that resveratrol has a lipophilic nature, thus its preferential localization should be in the nanoparticle's core. The same happens with the grape's extracts, even though they are constituted by hydrophilic and lipophilic compounds, the extracts were successfully encapsulated in the SLNs. Furthermore, no significant differences were found between the different nanoparticles ($P > 0.05$).

## 4.1.1 - Morphology

The morphology of the lipid nanoparticles was observed by TEM (Figure 4.3). The images revelled that generally the nanoparticles were almost spherical and with an uniform shape with smooth surfaces. TEM allowed confirming the sizes previously measured by DLS. Moreover, it is possible to observe that the nanoparticles shape did not seem to be altered when loaded with different compounds. Some aggregation was visible (Figure 4.3: C and E), however it could be due to the dilution rate of the formulation.

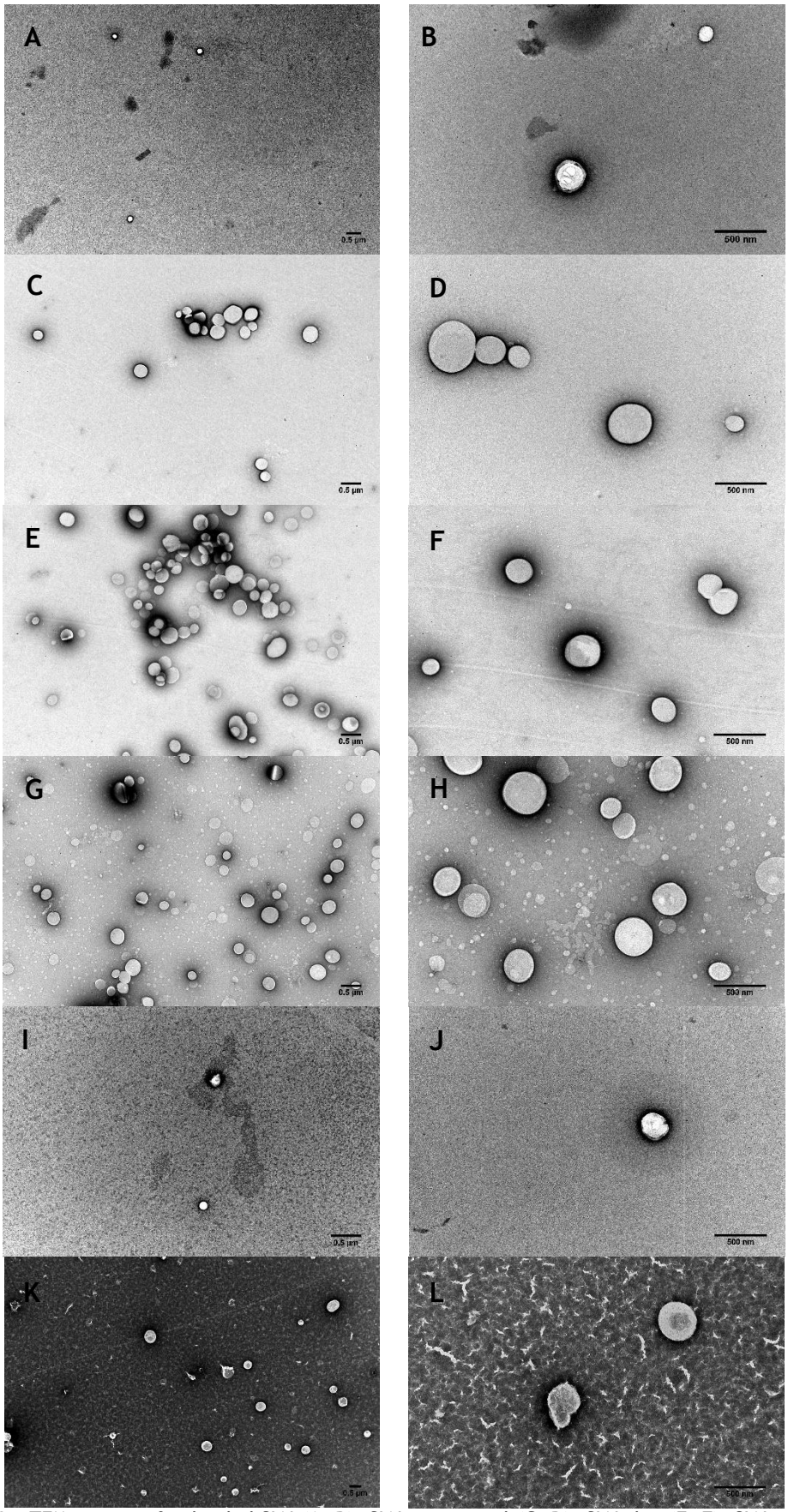


**Figure 4.3** – TEM images of unloaded SLN (A, B), SLN resveratrol (C, D), SLN skin (E, F), SLN centrifuged skin (G, H), SLN seeds (I, J) and SLN centrifuged seeds (K, L). Samples were diluted at a ratio of 1:100. Scale bar: 500 nm.

## 4.2 - Process yield

The process yield of the nanoparticles filtered through a 200 nm filter is 48±6%, which means that half of the nanoparticles constituents (lipids and/or drug) were lost during this process.

## 4.3 - Conjugation of the antibodies

For this experiment two types of lipid nanoparticles were developed. As a control, nanoparticles without conjugation with antibodies (mAb OX-26) were synthetised.

The binding of the mAb to the nanoparticles was determined by ELISA (Figure 4.4). Significantly higher absorbance at 405 nm was observed in the nanoparticles conjugated with mAbs when compared with the negative control and the nanoparticles without conjugation. Therefore, the antibody used demonstrate bioactivity for the transferrin receptor.

It is also important to refer that the thiolation of the mAbs does not interfere with their binding site [129], however the maleimide group can be hydrolysed when in contact with water, so it is highly recommended to conjugate the mAbs immediately after the nanoparticle synthesis.

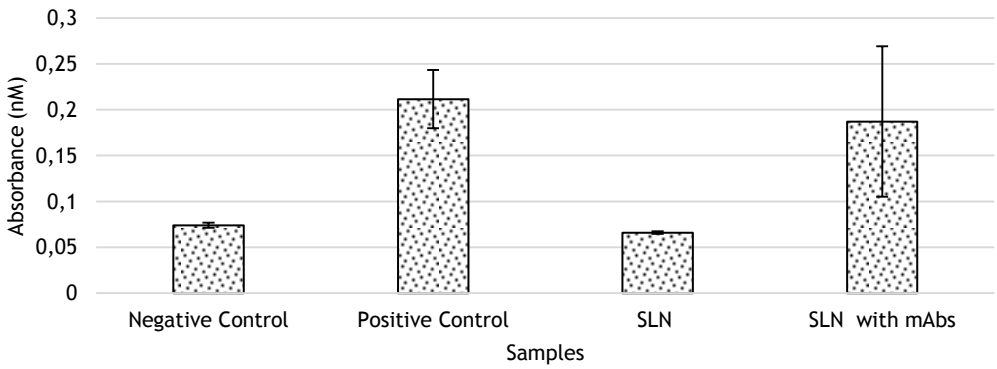


**Figure 4.4** - ELISA assay results of the negative (water) and positive control (OX-26), nanoparticles with and without conjugation with OX-26. All values represent the average and the standard deviation (n=2).

After conjugation, the nanoparticles size increased around 60 nm with no significance ($P > 0.05$) on the SLN skin, resveratrol and unloaded, and with significance on the SLN centrifuged skin, seeds and centrifuged seeds ($P < 0.05$). The size increase of the nanoparticles is an indicator if an efficient conjugation since the diameter of the globular antibody is approximately 15 nm [130]. However, and exaggerated increase could mean aggregation of the nanoparticles with is not desirable.

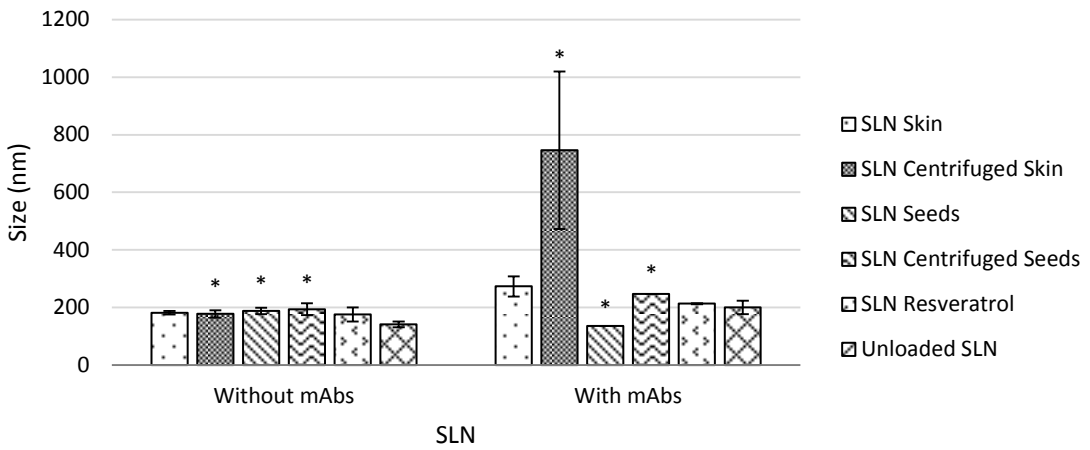


**Figure 4.5** – Comparison between the nanoparticles average size without and with antibodies. There are represented the sizes of SLN skin, SLN centrifuged skin, SLN seeds, SLN centrifuged seeds, SLN resveratrol and unloaded SLN. All values represent the average and the standard deviation (n=2).

## 4.4 - Solid lipid nanoparticle stability

After synthesis and after each month, the nanoparticle size was determined (Figure 4.6). Both average diameter and polidispersity index were used as an indication of nanoparticle aggregation and stability. For the majority of the formulations the average diameter increased during storage, however this increase was only statistically significant in few formulations when compared with the initial size ($P < 0.05$). Thus, although there was a slight increase of the size, it does not imply aggregation of the nanoparticles since the most of the nanoparticles still have less than 200 nm.

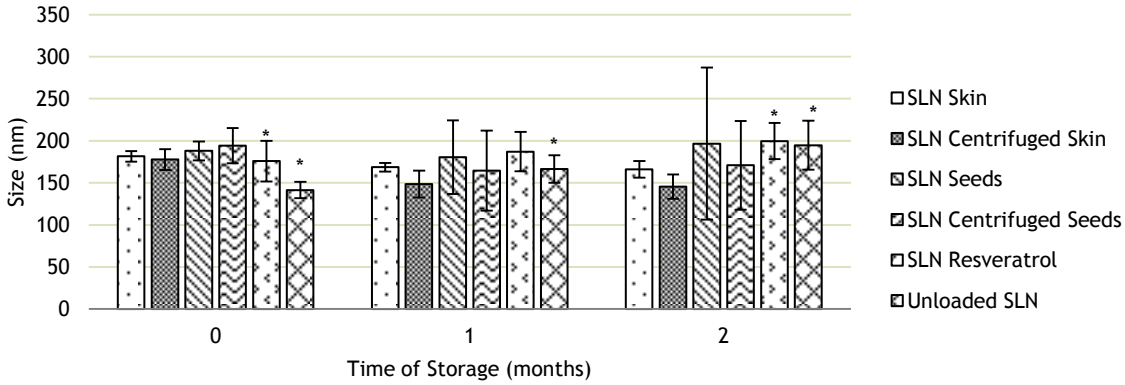


**Figure 4.6 -** Effect of the storage (at room temperature) on the nanoparticle size loaded with 10 mg of different compounds (grape's skin, grape's centrifuged skin, grape's seeds, grape's centrifuged seeds or resveratrol) and on the unloaded nanoparticles. Both SLN resveratrol and unloaded SLN were only studied until 1 month of storage. All values represent the average and the standard deviation (n=3).

On Table 4.3 is represented the effect of the storage on the SLN zeta potential of the different formulations. Since the values are not significantly different from each other, it is possible to affirm that the nanoparticles steric stability has not been affected by the storage time neither the storage conditions. This stability is corroborated by the maintenance of the nanoparticles size observed before.

**Table 4.3 -** Effect of the storage (at room temperature) on the nanoparticle zeta potential loaded with 10 mg of different compounds (grape's skin, grape's centrifuged skin, grape's seeds, grape's centrifuged seeds or resveratrol) and on the unloaded nanoparticles. Both SLN resveratrol and unloaded SLN were only studied until 1 month of storage. All values represent the average (n=3).

| SLN | Time of storage (months) | | |
|---|---|---|---|
| | **0** | **1** | **2** |
| **Unloaded** | -0.08 | 0.02 | -0.07 |
| **Resveratrol** | 0.19 | 0.02 | -0.06 |
| **Skin** | -0.07 | -0.14 | -0.02 |
| **Centrifuged Skin** | -0.09 | -0.04 | -0.15 |
| **Seeds** | 0.34 | -0.005 | -0.04 |
| **Centrifuged Seeds** | 0.02 | 0.06 | -0.09 |

One parameter to access the stability of the different formulations is the entrapment efficiency. It is know that SLN have a highly organized matrix with a tendency to from perfect crystals over time, which can eventually lead to an expulsion of the drug during the storage. However, the results of entrapment efficiency shown on Figure 4.7 contradict this hypothesis, demonstrating that the nanoparticles studies were able to retain the initial amount of encapsulated drug at least during 2 months. Only in one formulation statistically significance differences where observed between the final and initial time of storage ($P < 0.05$).

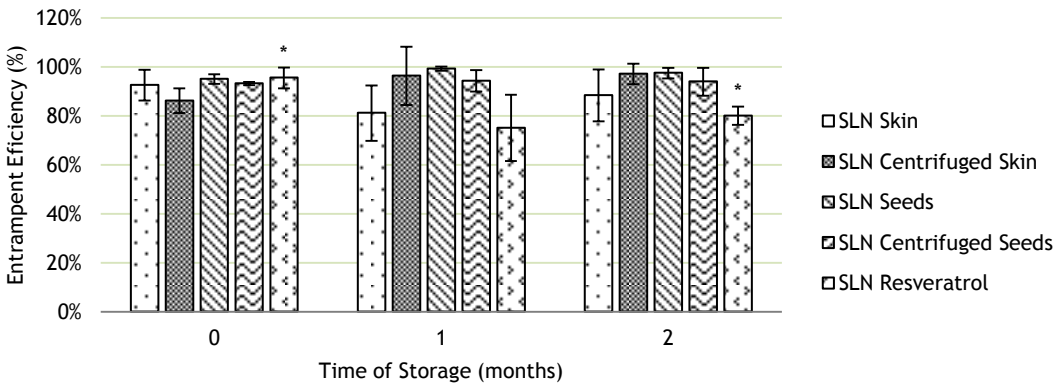


**Figure 4.7 -** Effect of the storage (at room temperature) on the nanoparticle entrapment efficiency loaded with 10 mg of different compounds (grape's skin, grape's centrifuged skin, grape's seeds, grape's centrifuged seeds or resveratrol) and on the unloaded nanoparticles. All values represent the average (n=3).

This stability study shows that the lipid nanoparticles synthesized resulted in a stable nanocarrier, which can be used as a controlled-release strategy for brain targeted delivery of both resveratrol and grape's extracts (skin and seeds).

## 4.5 - Effect of the loaded solid lipid nanoparticles on the α-synuclein and amyloid-β aggregation

In order to know how the different nanoparticles interact with α-synuclein and amyloid-β, specifically to know it they are able to prevent and/or reduce the aggregation of these peptides, two kinetics studies were made.

The results of the kinetic studies with amyloid-β are shown on Figure 4.8 (interaction with compounds) and Figure 4.9 (interaction with lipid nanoparticles). On Figure 4.8 is clear the both resveratrol and grape's extracts were able to inhibit the aggregation of amyloid-β, being the inhibition more accentuated when it interacts with resveratrol.

On the other hand, when these compounds are encapsulated it seems that the inhibition of the aggregation is diminished (Figure 4.9). This could be due to the difference of drug concentration on the different assays: the concentration of drug on the first one is the same as the theoretical concentration of the drug in the nanoparticles, without taking in account the yield of the filtering process. Moreover, is possible that the drug release did not achieve a considerable percentage of drug able to get out of the nanoparticles due to low degradation of the lipid nanoparticles. These results also shown that the unloaded nanoparticles acted as nucleus that promotes the aggregation of the amyloid-β peptide, since when both are incubated the value of fluorescence was higher than the amyloid-β incubated alone.

On Figure 4.10 the results of the interaction of the different lipid nanoparticles with α-synuclein peptide are presented. Although the formation of aggregates occurred, it is possible to notice a diminished fluorescence when the nanoparticles where incubated with the α-synuclein, leading to the conclusion that the different compound did indeed inhibited the aggregation potential of the α-synuclein.

Several studies indicate that the central region and the C-terminal tail of α-synuclein and amyloid-β are considered to have an important modulating role in the formation of pre-oligomers [131-133], thus peptide binding with these regions can prevent the formation of aggregates. Additionally, different mechanisms could be involved in the interaction of amyloid aggregates with both resveratrol and grape's extracts. Properties such as aromatic interactions, antioxidative activity, metal chelating and hydrogel binding can contribute to the inhibition of aggregates formation [134, 135].

Furthermore, resveratrol can intervene in the natural development of neurodegenerative diseases, preventing further neuronal deterioration [136]. The same applies to the grape's extracts, even if resveratrol is not the main constituent, its action results of synergic action of a mixture of many bioactive constituents, essentially polyphenols [134].

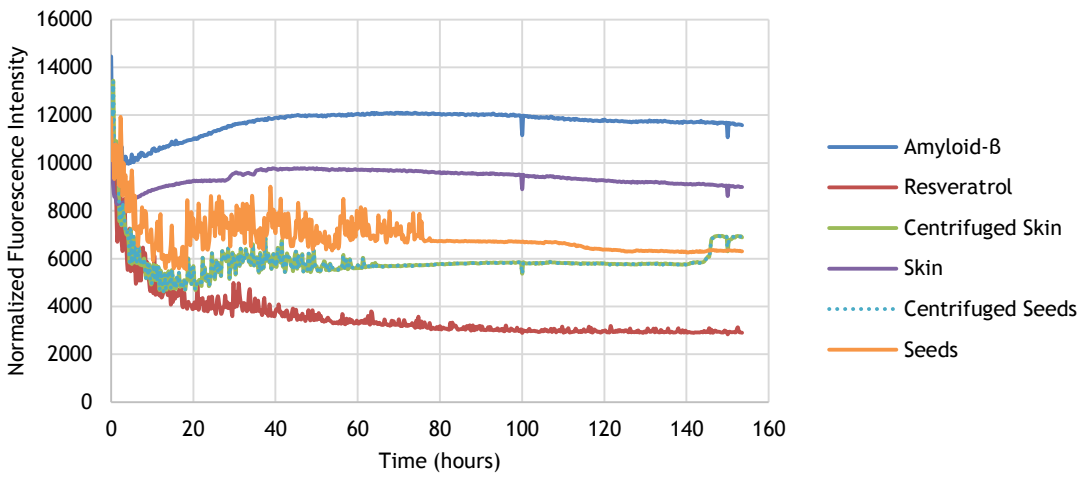


**Figure 4.8** - Kinetic study of the interaction of the free resveratrol and grape's extracts with the amyloid-β peptide using Thioflavin T.

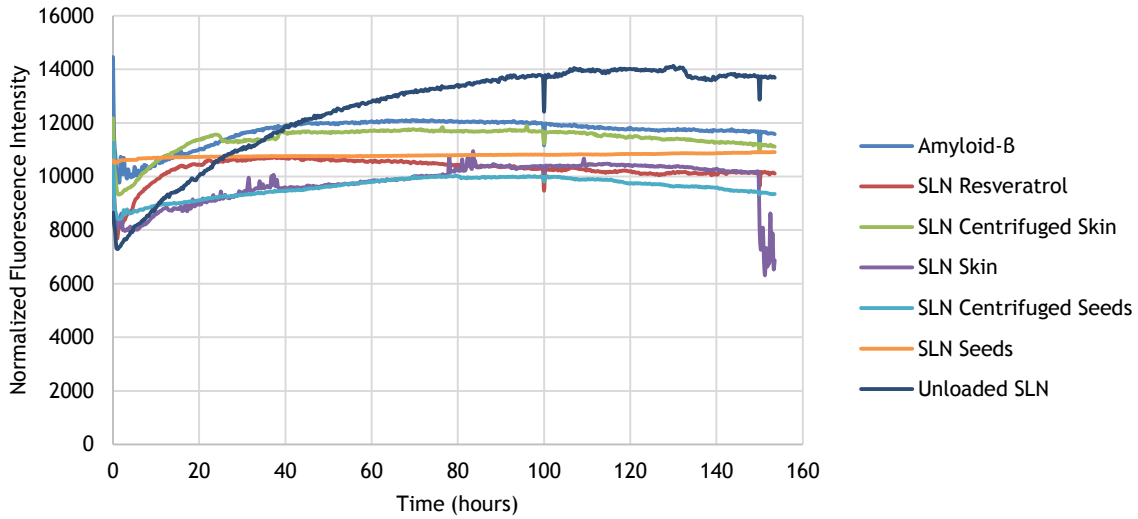


**Figure 4.9** - Kinetic study of the interaction of the loaded-nanoparticles (resveratrol and grape's extracts) and unloaded-nanoparticles with the amyloid-β peptide using Thioflavin T.

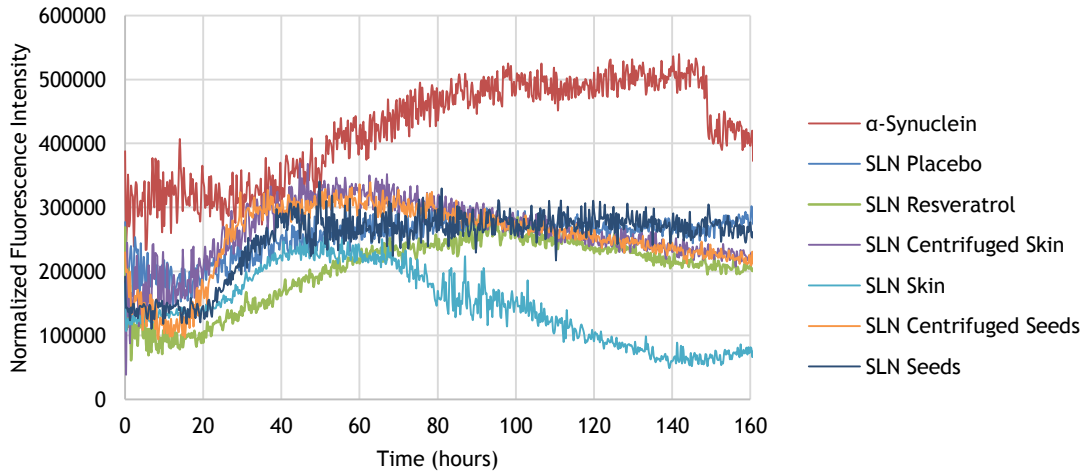


**Figure 4.10** - Kinetic study of the interaction of the loaded-nanoparticles (resveratrol and grape's extracts) and unloaded-nanoparticles with the α-synuclein peptide using Thioflavin T.

# Chapter 5

# Concluding remarks and future perspectives

Nowadays, neurodegenerative diseases are one of the major health problems in the world and, since there has been an increase of lifetime and aging of population, the number of neurodegenerative diseases also expected to increase in the near future. So it is clear the necessity of a new therapy for neurodegenerative diseases that affect the disease progression, rather than simply treating the symptoms. Nanotechnology has an important role on the development of an effective solution for the therapy of neurodegenerative disorders such as PD and AD through the drug delivery, neuroprotection or even though the regeneration of damaged neurons [7].

The use of nanoparticles to transport therapeutic drugs for both PD and AD, through non-invasive administration by intravenous injection, is an alluring method to avoid the long-term side-effects and peripheral toxicity associated to the relatively toxic drugs. Also, the effective brain drug delivery by the use of nanoparticles may reduce the necessary drug dosage, and will lead to an improvement of the patient's quality of life. Furthermore, they are able to transport a great variety of drugs across the BBB, including therapeutic drugs that were not used for treatment of these diseases due to their inability to cross this barrier in therapeutically effective concentrations [77]. However, it is necessary to give attention to the nanoparticle properties, like size, shape, geometry, charge, structure and composition, in order to guarantee the control of their fate in the *in vivo* environment [7].

In this work, the advantageous properties of both resveratrol and grape's extracts have been exploited by its encapsulation in lipid nanoparticles. These nanoparticles were functionalized with OX-26 antibodies to target the blood-brain barrier. Stability studies were performed to access the use of these SLN as promising future drug delivery systems, and the results showed that the nanoparticles are stable for a minimum period of two months without functionalization. However, when the coupling of the antibodies happened, the stability of the systems was greatly diminished, indicating that the process needs to be optimized to avoid the aggregation of the nanoparticles.

The interaction studies showed that the nanoparticles loaded with resveratrol or grape's extracts delayed and reduce the aggregation of α-synuclein or amyloid-β. Moreover, the synthesized nanoparticles exhibit high encapsulation efficiencies of the compounds studied, even after storage. Overall, the solid lipid nanoparticles are a promising dynamic system for the targeted delivery of grape's extracts, as a natural substitute of resveratrol, to the brain

in order to inhibit the formation of α-synuclein or amyloid-β aggregates, thus preventing, lowing the progression or even reverse both PD and AD.

The next steps involve the study of the release profile of the encapsulated molecules in an environment that simulated the blood stream and *in vitro* studies with BBB-models to confirm their ability to cross this barrier.

# References

[1] (UK) NCCfCC. Parkinson's Disease: National Clinical Guideline for Diagnosis and Management in Primary and Secondary Care. London: Royal College of Physicians (UK): NICE Clinical Guidelines; 2006.
[2] Baba M, Nakajo S, Tu P-H, Tomita T, Kazuyasu Nakaya, Lee VM-Y, et al. Aggregation of α-Synuclein in Lewy bodies of sporadic Parkinson's disease and dementia with Lewy bodies. American Journal of Pathology. 1998;154:879-84.
[3] Bekris LM, Yu CE, Bird TD, Tsuang DW. Genetics of Alzheimer disease. Journal of geriatric psychiatry and neurology. 2010;23:213-27.
[4] Lockman PR, Mumper RJ, Khan MA, Allen DD. Nanoparticle technology for drug delivery across the blood-brain barrier. Drug development and industrial pharmacy. 2002;28:1-13.
[5] De Rosa G, Salzano G, Caraglia M, Abbruzzese A. Nanotechnologies: A Strategy to Overcome Blood-Brain Barrier. Curr Drug Metab. 2012;13:61-9.
[6] Neves AR, Lucio M, Lima JL, Reis S. Resveratrol in medicinal chemistry: a critical review of its pharmacokinetics, drug-delivery, and membrane interactions. Current medicinal chemistry. 2012;19:1663-81.
[7] Pehlivan SB. Nanotechnology-based drug delivery systems for targeting, imaging and diagnosis of neurodegenerative diseases. Pharmaceutical research. 2013;30:2499-511.
[8] Gundersen V. Protein aggregation in Parkinson's disease. Acta Neurologia Scandinavica. 2010;122:82-7.
[9] Olanow CW, Tatton WG. Etiology and pathogenesis of Parkinson's disease. Annual review of neuroscience. 1999;22:123-44.
[10] van Rooden SM, Heiser WJ, Kok JN, Verbaan D, van Hilten JJ, Marinus J. The identification of Parkinson's disease subtypes using cluster analysis: a systematic review. Movement disorders : official journal of the Movement Disorder Society. 2010;25:969-78.
[11] McCann H, Stevens CH, Cartwright H, Halliday GM. alpha-Synucleinopathy phenotypes. Parkinsonism & related disorders. 2014;20 Suppl 1:S62-7.
[12] Navarro JA, Hessner S, Yenisetti SC, Bayersdorfer F, Zhang L, Voigt A, et al. Analysis of dopaminergic neuronal dysfunction in genetic and toxin-induced models of Parkinson's disease in Drosophila. Journal of neurochemistry. 2014;131:369-82.
[13] Trojanowski JQ, Lee VM. Aggregation of neurofilament and alpha-synuclein proteins in Lewy bodies: implications for the pathogenesis of Parkinson disease and Lewy body dementia. Archives of neurology. 1998;55:151-2.
[14] Savitt JM, Dawson VL, Dawson TM. Diagnosis and treatment of Parkinson disease: molecules to medicine. The Journal of clinical investigation. 2006;116:1744-54.
[15] Shulman JM, De Jager PL, Feany MB. Parkinson's disease: genetics and pathogenesis. Annual review of pathology. 2011;6:193-222.
[16] Spillantini MG, Schmidt ML, Lee VM, Trojanowski JQ, Jakes R, Goedert M. Alpha-synuclein in Lewy bodies. Nature. 1997;388:839-40.
[17] Yadav S, Dixit A, Agrawal S, Singh A, Srivastava G, Singh AK, et al. Rodent models and contemporary molecular techniques: notable feats yet incomplete explanations of Parkinson's disease pathogenesis. Molecular neurobiology. 2012;46:495-512.
[18] Breydo L, Wu JW, Uversky VN. Alpha-synuclein misfolding and Parkinson's disease. Biochimica et biophysica acta. 2012;1822:261-85.
[19] Miller DB, O'Callaghan JP. Biomarkers of Parkinson's disease (PD): Present and future. Metabolism: clinical and experimental. 2014.

[20] Johnson ME, Bobrovskaya L. An update on the rotenone models of Parkinson's disease: Their ability to reproduce the features of clinical disease and model gene-environment interactions. Neurotoxicology. 2014.
[21] Hawkes CH, Del Tredici K, Braak H. Parkinson's disease: a dual-hit hypothesis. Neuropathology and applied neurobiology. 2007;33:599-614.
[22] Braak H, Del Tredici K, Rub U, de Vos RA, Jansen Steur EN, Braak E. Staging of brain pathology related to sporadic Parkinson's disease. Neurobiology of aging. 2003;24:197-211.
[23] Bhidayasiri R, Truong DD. Therapeutic strategies for nonmotor symptoms in early Parkinson's disease: the case for a higher priority and stronger evidence. Parkinsonism & related disorders. 2012;18 Suppl 1:S110-3.
[24] Jakes R, Spillantini MG, Goedert M. Identification of two distinct synucleins from human brain. FEBS letters. 1994;345:27-32.
[25] Dickson DW. Parkinson's disease and parkinsonism: neuropathology. Cold Spring Harbor perspectives in medicine. 2012;2.
[26] Spillantini MG, Crowther RA, Jakes R, Hasegawa M, Goedert M. alpha-Synuclein in filamentous inclusions of Lewy bodies from Parkinson's disease and dementia with lewy bodies. Proceedings of the National Academy of Sciences of the United States of America. 1998;95:6469-73.
[27] Stefanis L. alpha-Synuclein in Parkinson's disease. Cold Spring Harbor perspectives in medicine. 2012;2:a009399.
[28] Barbour R, Kling K, Anderson JP, Banducci K, Cole T, Diep L, et al. Red blood cells are the major source of alpha-synuclein in blood. Neuro-degenerative diseases. 2008;5:55-9.
[29] Kahle PJ. alpha-Synucleinopathy models and human neuropathology: similarities and differences. Acta neuropathologica. 2008;115:87-95.
[30] George JM. The synucleins. Genome biology. 2002;3:REVIEWS3002.
[31] Uversky VN. A protein-chameleon: conformational plasticity of alpha-synuclein, a disordered protein involved in neurodegenerative disorders. Journal of biomolecular structure & dynamics. 2003;21:211-34.
[32] Lashuel HA, Overk CR, Oueslati A, Masliah E. The many faces of alpha-synuclein: from structure and toxicity to therapeutic target. Nature reviews Neuroscience. 2013;14:38-48.
[33] Orcellet ML, Fernandez CO. Structures behind the amyloid aggregation of alpha-synuclein: an NMR based approach. Current protein & peptide science. 2011;12:188-204.
[34] Kakish J, Tavassoly O, Lee JS. Rasagiline, a Suicide Inhibitor of Monoamine Oxidases, Binds Reversibly to alpha-Synuclein. ACS chemical neuroscience. 2014.
[35] Bousset L, Pieri L, Ruiz-Arlandis G, Gath J, Jensen PH, Habenstein B, et al. Structural and functional characterization of two alpha-synuclein strains. Nature communications. 2013;4:2575.
[36] Kaur IP, Bhandari R, Bhandari S, Kakkar V. Potential of solid lipid nanoparticles in brain targeting. Journal of controlled release : official journal of the Controlled Release Society. 2008;127:97-109.
[37] Dickson DW, Uchikado H, Fujishiro H, Tsuboi Y. Evidence in favor of Braak staging of Parkinson's disease. Movement disorders : official journal of the Movement Disorder Society. 2010;25 Suppl 1:S78-82.
[38] Irwin DJ, Lee VM, Trojanowski JQ. Parkinson's disease dementia: convergence of alpha-synuclein, tau and amyloid-beta pathologies. Nature reviews Neuroscience. 2013;14:626-36.
[39] Poewe W, Antonini A, Zijlmans JCM, Burkhard PR, Vingerhoets F. Levodopa in the treatment of Parkinson's disease: an old drug still going strong. Clin Interv Aging. 2010;5:229-38.
[40] Garbayo E, Ansorena E, Blanco-Prieto MJ. Drug development in Parkinson's disease: from emerging molecules to innovative drug delivery systems. Maturitas. 2013;76:272-8.
[41] Kulisevsky J, Luquin MR, Arbelo JM, Burguera JA, Carrillo F, Castro A, et al. Advanced Parkinson's disease: clinical characteristics and treatment. Part II. Neurologia. 2013;28:558-83.
[42] Stocchi F. Therapy for Parkinson's disease: what is in the pipeline? Neurotherapeutics : the journal of the American Society for Experimental NeuroTherapeutics. 2014;11:24-33.
[43] Rascol O, Lozano A, Stern M, Poewe W. Milestones in Parkinson's disease therapeutics. Movement disorders : official journal of the Movement Disorder Society. 2011;26:1072-82.

[44] Gao HL, Pang ZQ, Jiang XG. Targeted Delivery of Nano-Therapeutics for Major Disorders of the Central Nervous System. Pharmaceutical research. 2013;30:2485-98.
[45] Stayte S, Vissel B. Advances in non-dopaminergic treatments for Parkinson's disease. Frontiers in neuroscience. 2014;8:113.
[46] Kumar A, Singh A, Ekavali. A review on Alzheimer's disease pathophysiology and its management: an update. Pharmacological reports : PR. 2015;67:195-203.
[47] Forstl H, Kurz A. Clinical features of Alzheimer's disease. European archives of psychiatry and clinical neuroscience. 1999;249:288-90.
[48] Larson EB, Shadlen MF, Wang L, McCormick WC, Bowen JD, Teri L, et al. Survival after initial diagnosis of Alzheimer disease. Annals of internal medicine. 2004;140:501-9.
[49] Anekonda TS. Resveratrol--a boon for treating Alzheimer's disease? Brain research reviews. 2006;52:316-26.
[50] Salawu FK, Umar JT, Olokoba AB. Alzheimer's disease: a review of recent developments. Annals of African medicine. 2011;10:73-9.
[51] Markus MA, Morris BJ. Resveratrol in prevention and treatment of common clinical conditions of aging. Clin Interv Aging. 2008;3:331-9.
[52] Seubert P, Oltersdorf T, Lee MG, Barbour R, Blomquist C, Davis DL, et al. Secretion of beta-amyloid precursor protein cleaved at the amino terminus of the beta-amyloid peptide. Nature. 1993;361:260-3.
[53] Kirschner DA, Abraham C, Selkoe DJ. X-ray diffraction from intraneuronal paired helical filaments and extraneuronal amyloid fibers in Alzheimer disease indicates cross-beta conformation. Proceedings of the National Academy of Sciences of the United States of America. 1986;83:503-7.
[54] Ladiwala AR, Litt J, Kane RS, Aucoin DS, Smith SO, Ranjan S, et al. Conformational differences between two amyloid beta oligomers of similar size and dissimilar toxicity. The Journal of biological chemistry. 2012;287:24765-73.
[55] Gouras GK, Almeida CG, Takahashi RH. Intraneuronal Abeta accumulation and origin of plaques in Alzheimer's disease. Neurobiology of aging. 2005;26:1235-44.
[56] Hardy J, Selkoe DJ. The amyloid hypothesis of Alzheimer's disease: progress and problems on the road to therapeutics. Science. 2002;297:353-6.
[57] Kang J, Lemaire HG, Unterbeck A, Salbaum JM, Masters CL, Grzeschik KH, et al. The precursor of Alzheimer's disease amyloid A4 protein resembles a cell-surface receptor. Nature. 1987;325:733-6.
[58] Haass C, Schlossmacher MG, Hung AY, Vigo-Pelfrey C, Mellon A, Ostaszewski BL, et al. Amyloid beta-peptide is produced by cultured cells during normal metabolism. Nature. 1992;359:322-5.
[59] Jarrett JT, Berger EP, Lansbury PT, Jr. The carboxy terminus of the beta amyloid protein is critical for the seeding of amyloid formation: implications for the pathogenesis of Alzheimer's disease. Biochemistry. 1993;32:4693-7.
[60] Hardy JA, Higgins GA. Alzheimer's disease: the amyloid cascade hypothesis. Science. 1992;256:184-5.
[61] Shankar GM, Li S, Mehta TH, Garcia-Munoz A, Shepardson NE, Smith I, et al. Amyloid-beta protein dimers isolated directly from Alzheimer's brains impair synaptic plasticity and memory. Nature medicine. 2008;14:837-42.
[62] Mattson MP. Cellular actions of beta-amyloid precursor protein and its soluble and fibrillogenic derivatives. Physiological reviews. 1997;77:1081-132.
[63] Sun N, Funke SA, Willbold D. A survey of peptides with effective therapeutic potential in Alzheimer's disease rodent models or in human clinical studies. Mini reviews in medicinal chemistry. 2012;12:388-98.
[64] Skovronsky DM, Lee VM, Trojanowski JQ. Neurodegenerative diseases: new concepts of pathogenesis and their therapeutic implications. Annual review of pathology. 2006;1:151-70.
[65] Bartus RT, Emerich DF. Cholinergic markers in Alzheimer disease. Jama. 1999;282:2208-9.
[66] Auld DS, Kornecook TJ, Bastianetto S, Quirion R. Alzheimer's disease and the basal forebrain cholinergic system: relations to beta-amyloid peptides, cognition, and treatment strategies. Progress in neurobiology. 2002;68:209-45.
[67] Jahn TR, Radford SE. The Yin and Yang of protein folding. The FEBS journal. 2005;272:5962-70.

[68] Merlini G, Bellotti V. Molecular mechanisms of amyloidosis. The New England journal of medicine. 2003;349:583-96.
[69] Selkoe DJ. Alzheimer's disease: genes, proteins, and therapy. Physiological reviews. 2001;81:741-66.
[70] Hardy J. The Alzheimer family of diseases: many etiologies, one pathogenesis? Proceedings of the National Academy of Sciences of the United States of America. 1997;94:2095-7.
[71] Wolfe ML, Rader DJ. Cholesteryl ester transfer protein and coronary artery disease: an observation with therapeutic implications. Circulation. 2004;110:1338-40.
[72] Bird TD. Alzheimer Disease Overview. In: Pagon RA, Adam MP, Ardinger HH, Wallace SE, Amemiya A, Bean LJH, et al., editors. GeneReviews(R). Seattle (WA)1993.
[73] Forman MS, Trojanowski JQ, Lee VM. Neurodegenerative diseases: a decade of discoveries paves the way for therapeutic breakthroughs. Nature medicine. 2004;10:1055-63.
[74] Abbott NJ, Patabendige AA, Dolman DE, Yusof SR, Begley DJ. Structure and function of the blood-brain barrier. Neurobiology of disease. 2010;37:13-25.
[75] Liebner S, Czupalla CJ, Wolburg H. Current concepts of blood-brain barrier development. The International journal of developmental biology. 2011;55:467-76.
[76] Cardoso FL, Brites D, Brito MA. Looking at the blood–brain barrier: Molecular anatomy and possible investigation approaches. Brain research reviews. 2010;64:328-63.
[77] Wohlfart S, Gelperina S, Kreuter J. Transport of drugs across the blood-brain barrier by nanoparticles. Journal of controlled release : official journal of the Controlled Release Society. 2012;161:264-73.
[78] Pardridge WM. Drug transport across the blood-brain barrier. Journal of cerebral blood flow and metabolism : official journal of the International Society of Cerebral Blood Flow and Metabolism. 2012;32:1959-72.
[79] Rosenberg GA. Neurological diseases in relation to the blood-brain barrier. Journal of cerebral blood flow and metabolism : official journal of the International Society of Cerebral Blood Flow and Metabolism. 2012;32:1139-51.
[80] Krol S. Challenges in drug delivery to the brain: Nature is against us. Journal of Controlled Release. 2012;164:145-55.
[81] Wilhelm I, Fazakas C, Krizbai IA. In vitro models of the blood-brain barrier. Acta neurobiologiae experimentalis. 2011;71:113-28.
[82] Schroeder U, Sommerfeld P, Ulrich S, Sabel BA. Nanoparticle Technology for Delivery of Drugs Across the Blood-Brain Barrier. Journal of Pharmaceutical Sciences. 1998;87:3.
[83] Chen Y, Liu L. Modern methods for delivery of drugs across the blood-brain barrier. Advanced drug delivery reviews. 2012;64:640-65.
[84] Masserini M. Nanoparticles for Brain Drug Delivery. ISRN Biochemistry. 2013;2013:18.
[85] Trapani A, De Giglio E, Cafagna D, Denora N, Agrimi G, Cassano T, et al. Characterization and evaluation of chitosan nanoparticles for dopamine brain delivery. Int J Pharm. 2011;419:296-307.
[86] Peura L, Malmioja K, Huttunen K, Leppanen J, Hamalainen M, Forsberg MM, et al. Design, synthesis and brain uptake of LAT1-targeted amino acid prodrugs of dopamine. Pharmaceutical research. 2013;30:2523-37.
[87] Pillay S, Pillay V, Choonara YE, Naidoo D, Khan RA, du Toit LC, et al. Design, biometric simulation and optimization of a nano-enabled scaffold device for enhanced delivery of dopamine to the brain. Int J Pharm. 2009;382:277-90.
[88] During MJ, Freese A, Deutch AY, Kibat PG, Sabel BA, Langer R, et al. Biochemical and behavioral recovery in a rodent model of Parkinson's disease following stereotactic implantation of dopamine-containing liposomes. Exp Neurol. 1992;115:193-9.
[89] Malvindi MA, Di Corato R, Curcio A, Melisi D, Rimoli MG, Tortiglione C, et al. Multiple functionalization of fluorescent nanoparticles for specific biolabeling and drug delivery of dopamine. Nanoscale. 2011;3:5110-9.
[90] Garbayo E, Montero-Menei CN, Ansorena E, Lanciego JL, Aymerich MS, Blanco-Prieto MJ. Effective GDNF brain delivery using microspheres--a promising strategy for Parkinson's disease. Journal of controlled release : official journal of the Controlled Release Society. 2009;135:119-26.

[91] Huang R, Ke W, Liu Y, Wu D, Feng L, Jiang C, et al. Gene therapy using lactoferrin-modified nanoparticles in a rotenone-induced chronic Parkinson model. J Neurol Sci. 2010;290:123-30.
[92] Gujral C, Minagawa Y, Fujimoto K, Kitano H, Nakaji-Hirabayashi T. Biodegradable microparticles for strictly regulating the release of neurotrophic factors. Journal of controlled release : official journal of the Controlled Release Society. 2013;168:307-16.
[93] Lampe KJ, Kern DS, Mahoney MJ, Bjugstad KB. The administration of BDNF and GDNF to the brain via PLGA microparticles patterned within a degradable PEG-based hydrogel: Protein distribution and the glial response. J Biomed Mater Res A. 2011;96:595-607.
[94] Herran E, Ruiz-Ortega JA, Aristieta A, Igartua M, Requejo C, Lafuente JV, et al. In vivo administration of VEGF- and GDNF-releasing biodegradable polymeric microspheres in a severe lesion model of Parkinson's disease. Eur J Pharm Biopharm. 2013;85:1183-90.
[95] Delcroix GJ, Garbayo E, Sindji L, Thomas O, Vanpouille-Box C, Schiller PC, et al. The therapeutic potential of human multipotent mesenchymal stromal cells combined with pharmacologically active microcarriers transplanted in hemi-parkinsonian rats. Biomaterials. 2011;32:1560-73.
[96] Yurek DM, Flectcher AM, Kowalczyk TH, Padegimas L, Cooper MJ. Compacted DNA nanoparticle gene transfer of GDNF to the rat striatum enhances the survival of grafted fetal dopamine neurons. Cell Transplant. 2009;18:1183-96.
[97] Woerly S, Fort S, Pignot-Paintrand I, Cottet C, Carcenac C, Savasta M. Development of a sialic acid-containing hydrogel of poly[N-(2-hydroxypropyl) methacrylamide]: characterization and implantation study. Biomacromolecules. 2008;9:2329-37.
[98] D'Aurizio E, Sozio P, Cerasa LS, Vacca M, Brunetti L, Orlando G, et al. Biodegradable microspheres loaded with an anti-Parkinson prodrug: an in vivo pharmacokinetic study. Mol Pharm. 2011;8:2408-15.
[99] Ren T, Yang X, Wu N, Cai Y, Liu Z, Yuan W. Sustained-release formulation of levodopa methyl ester/benserazide for prolonged suppressing dyskinesia expression in 6-OHDA-leisoned rats. Neurosci Lett. 2011;502:117-22.
[100] Yang X, Zheng R, Cai Y, Liao M, Yuan W, Liu Z. Controlled-release levodopa methyl ester/benserazide-loaded nanoparticles ameliorate levodopa-induced dyskinesia in rats. International journal of nanomedicine. 2012;7:2077-86.
[101] Sharma S, Lohan S, Murthy RS. Formulation and characterization of intranasal mucoadhesive nanoparticulates and thermo-reversible gel of levodopa for brain delivery. Drug development and industrial pharmacy. 2014;40:869-78.
[102] Xiang Y, Wu Q, Liang L, Wang X, Wang J, Zhang X, et al. Chlorotoxin-modified stealth liposomes encapsulating levodopa for the targeting delivery against Parkinson's disease in the MPTP-induced mice model. Journal of drug targeting. 2012;20:67-75.
[103] Wang A, Wang L, Sun K, Liu W, Sha C, Li Y. Preparation of rotigotine-loaded microspheres and their combination use with L-DOPA to modify dyskinesias in 6-OHDA-lesioned rats. Pharmaceutical research. 2012;29:2367-76.
[104] Regnier-Delplace C, Thillaye du Boullay O, Siepmann F, Martin-Vaca B, Degrave N, Demonchaux P, et al. PLGA microparticles with zero-order release of the labile anti-Parkinson drug apomorphine. Int J Pharm. 2013;443:68-79.
[105] Tsai MJ, Huang YB, Wu PC, Fu YS, Kao YR, Fang JY, et al. Oral apomorphine delivery from solid lipid nanoparticles with different monostearate emulsifiers: pharmacokinetic and behavioral evaluations. J Pharm Sci. 2011;100:547-57.
[106] Azeem A, Talegaonkar S, Negi LM, Ahmad FJ, Khar RK, Iqbal Z. Oil based nanocarrier system for transdermal delivery of ropinirole: a mechanistic, pharmacokinetic and biochemical investigation. Int J Pharm. 2012;422:436-44.
[107] Md S, Khan RA, Mustafa G, Chuttani K, Baboota S, Sahni JK, et al. Bromocriptine loaded chitosan nanoparticles intended for direct nose to brain delivery: pharmacodynamic, pharmacokinetic and scintigraphy study in mice model. European journal of pharmaceutical sciences : official journal of the European Federation for Pharmaceutical Sciences. 2013;48:393-405.
[108] Gastaldi L, Battaglia L, Peira E, Chirio D, Muntoni E, Solazzi I, et al. Solid lipid nanoparticles as vehicles of drugs to the brain: Current state of the art. Eur J Pharm Biopharm. 2014;87:433-44.

[109] Carroll RT, Bhatia D, Geldenhuys W, Bhatia R, Miladore N, Bishayee A, et al. Brain-targeted delivery of Tempol-loaded nanoparticles for neurological disorders. Journal of drug targeting. 2010;18:665-74.
[110] Fernandez M, Barcia E, Fernandez-Carballido A, Garcia L, Slowing K, Negro S. Controlled release of rasagiline mesylate promotes neuroprotection in a rotenone-induced advanced model of Parkinson's disease. Int J Pharm. 2012;438:266-78.
[111] Hu K, Shi Y, Jiang W, Han J, Huang S, Jiang X. Lactoferrin conjugated PEG-PLGA nanoparticles for brain delivery: preparation, characterization and efficacy in Parkinson's disease. Int J Pharm. 2011;415:273-83.
[112] Wen Z, Yan Z, Hu K, Pang Z, Cheng X, Guo L, et al. Odorranalectin-conjugated nanoparticles: preparation, brain delivery and pharmacodynamic study on Parkinson's disease following intranasal administration. Journal of controlled release : official journal of the Controlled Release Society. 2011;151:131-8.
[113] Kurakhmaeva KB, Djindjikhashvili IA, Petrov VE, Balabanyan VU, Voronina TA, Trofimov SS, et al. Brain targeting of nerve growth factor using poly(butyl cyanoacrylate) nanoparticles. Journal of drug targeting. 2009;17:564-74.
[114] Mufamadi MS, Choonara YE, Kumar P, Modi G, Naidoo D, Ndesendo VM, et al. Surface-engineered nanoliposomes by chelating ligands for modulating the neurotoxicity associated with beta-amyloid aggregates of Alzheimer's disease. Pharmaceutical research. 2012;29:3075-89.
[115] Mathew A, Fukuda T, Nagaoka Y, Hasumura T, Morimoto H, Yoshida Y, et al. Curcumin loaded-PLGA nanoparticles conjugated with Tet-1 peptide for potential use in Alzheimer's disease. PLoS One. 2012;7:e32616.
[116] Esposito E, Fantin M, Marti M, Drechsler M, Paccamiccio L, Mariani P, et al. Solid lipid nanoparticles as delivery systems for bromocriptine. Pharmaceutical research. 2008;25:1521-30.
[117] Re F, Cambianica I, Sesana S, Salvati E, Cagnotto A, Salmona M, et al. Functionalization with ApoE-derived peptides enhances the interaction with brain capillary endothelial cells of nanoliposomes binding amyloid-beta peptide. J Biotechnol. 2010;156:341-6.
[118] Gokce EH, Korkmaz E, Dellera E, Sandri G, Bonferoni MC, Ozer O. Resveratrol-loaded solid lipid nanoparticles versus nanostructured lipid carriers: evaluation of antioxidant potential for dermal applications. International journal of nanomedicine. 2012;7:1841-50.
[119] de Boer AG, Gaillard PJ. Drug targeting to the brain. Annual review of pharmacology and toxicology. 2007;47:323-55.
[120] van Rooy I, Mastrobattista E, Storm G, Hennink WE, Schiffelers RM. Comparison of five different targeting ligands to enhance accumulation of liposomes into the brain. Journal of controlled release : official journal of the Controlled Release Society. 2011;150:30-6.
[121] Lajoie JM, Shusta EV. Targeting receptor-mediated transport for delivery of biologics across the blood-brain barrier. Annual review of pharmacology and toxicology. 2015;55:613-31.
[122] Ramalho MJA. PLGA Nanoparticles as a platform for Vitamin D-based cancer therapy. Porto: University of Porto; 2014.
[123] Tscharnuter W. Photon Correlation Spectroscopy in Particle Sizing. Encyclopedia of Analytical Chemistry: John Wiley & Sons, Ltd; 2006.
[124] Freire JM, Domingues MM, Matos J, Melo MN, Veiga AS, Santos NC, et al. Using zeta-potential measurements to quantify peptide partition to lipid membranes. European Biophysics Journal. 2011;40:481-7.
[125] Honary S, Zahir F. Effect of zeta potential on the properties of nano-drug delivery systems-a review (Part 2). Tropical Journal of Pharmaceutical Research. 2013;12:8.
[126] Loureiro J. Fluorinated peptides and functionalized liposomes to target amyloid deposits in Alzheimer's disease. Porto: University of Porto; 2013.
[127] Martins S, Tho I, Souto E, Ferreira D, Brandl M. Multivariate design for the evaluation of lipid and surfactant composition effect for optimisation of lipid nanoparticles. European journal of pharmaceutical sciences : official journal of the European Federation for Pharmaceutical Sciences. 2012;45:613-23.
[128] Iacopini P, Baldi M, Storchi P, Sebastiani L. Catechin, epicatechin, quercetin, rutin and resveratrol in red grape: Content, in vitro antioxidant activity and interactions. Journal of Food Composition and Analysis. 2008;21:589-98.

[129] Pardridge WM, Kang YS, Buciak JL, Yang J. Human insulin receptor monoclonal antibody undergoes high affinity binding to human brain capillaries in vitro and rapid transcytosis through the blood-brain barrier in vivo in the primate. Pharmaceutical research. 1995;12:807-16.
[130] Dammer U, Hegner M, Anselmetti D, Wagner P, Dreier M, Huber W, et al. Specific antigen/antibody interactions measured by force microscopy. Biophysical journal. 1996;70:2437-41.
[131] Ahn JS, Lee JH, Kim JH, Paik SR. Novel method for quantitative determination of amyloid fibrils of alpha-synuclein and amyloid beta/A4 protein by using resveratrol. Analytical biochemistry. 2007;367:259-65.
[132] Sivanesam K, Byrne A, Bisaglia M, Bubacco L, Andersen N. Binding Interactions of Agents That Alter alpha-Synuclein Aggregation. RSC advances. 2015;5:11577-90.
[133] Jayasena UL, Gribble SK, McKenzie A, Beyreuther K, Masters CL, Underwood JR. Identification of structural variations in the carboxyl terminus of Alzheimer's disease-associated beta A4[1-42] amyloid using a monoclonal antibody. Clin Exp Immunol. 2001;124:297-305.
[134] Gazova Z, Siposova K, Kurin E, Mucaji P, Nagy M. Amyloid aggregation of lysozyme: the synergy study of red wine polyphenols. Proteins. 2013;81:994-1004.
[135] Ge JF, Qiao JP, Qi CC, Wang CW, Zhou JN. The binding of resveratrol to monomer and fibril amyloid beta. Neurochemistry international. 2012;61:1192-201.
[136] Saiko P, Szakmary A, Jaeger W, Szekeres T. Resveratrol and its analogs: defense against cancer, coronary disease and neurodegenerative maladies or just a fad? Mutation research. 2008;658:68-94.

# Annex A

# Calibration Curves

The calibration curves of the grape's extracts were read at the wavelength of 278.5 nm and the extrapolations were made in mg of extract per mL of solution on a V-660 spectrophotometer (Jasco, Easton, MD, USA).

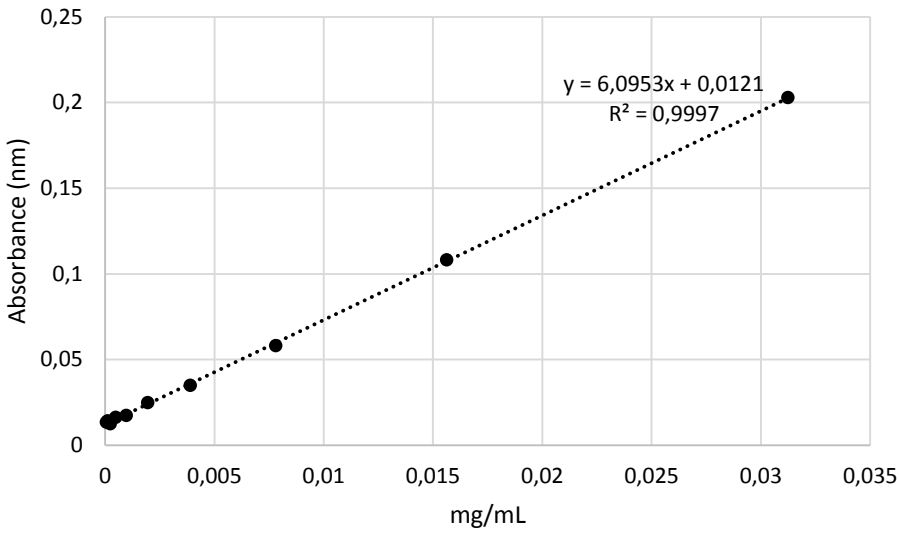


**Figure A.2** - Calibration curve of grape's skin.

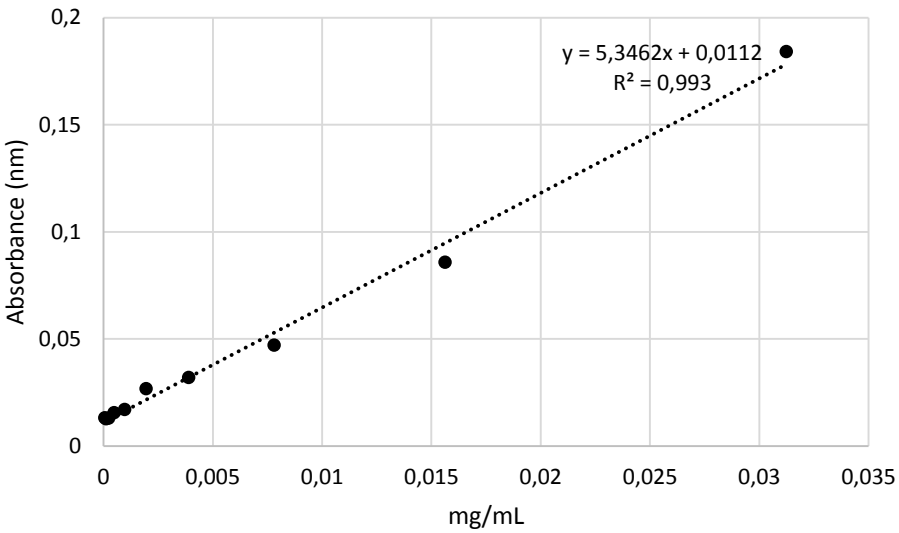


**Figure A.1** - Calibration curve of grape's centrifuged skin.

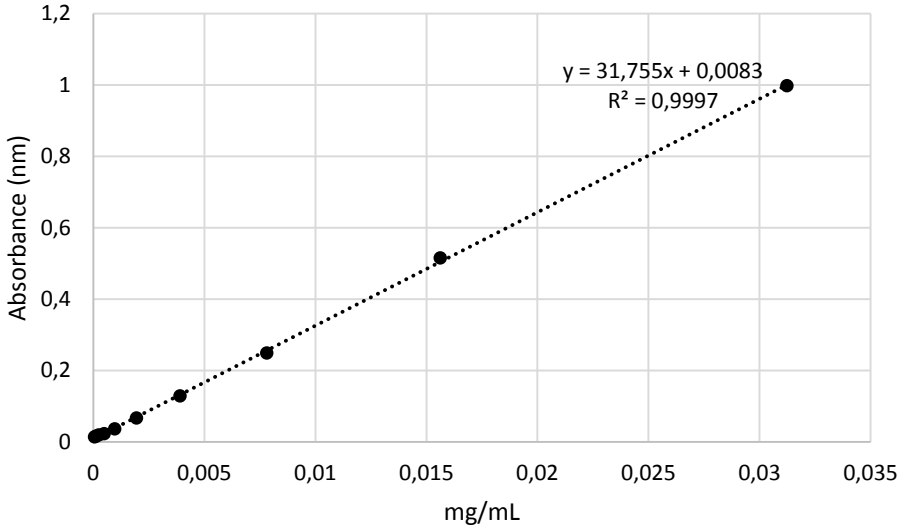


**Figure A.3 -** Calibration curve of grape's seeds.

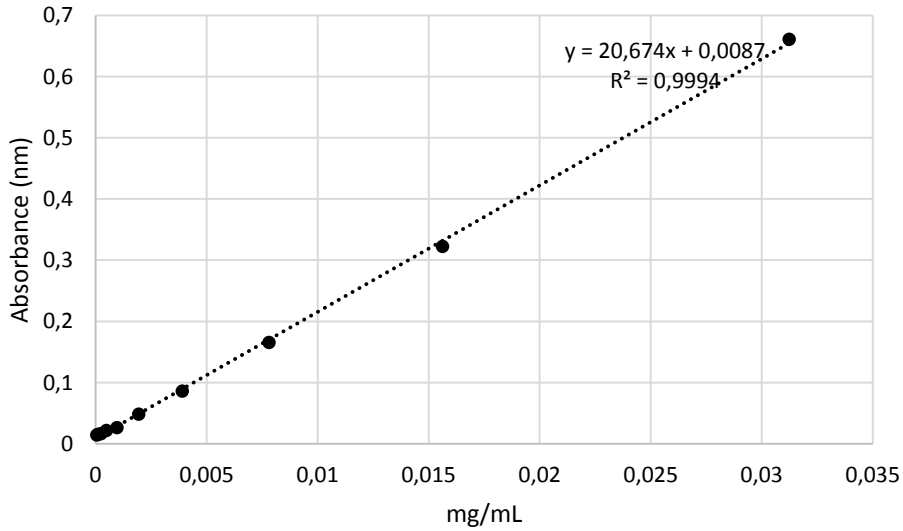


**Figure A.4 -** Calibration curve of grape's centrifuged seeds.

The calibration curve for resveratrol was read at the wavelength of 305 nm on a V-660 spectrophotometer (Jasco, Easton, MD, USA).

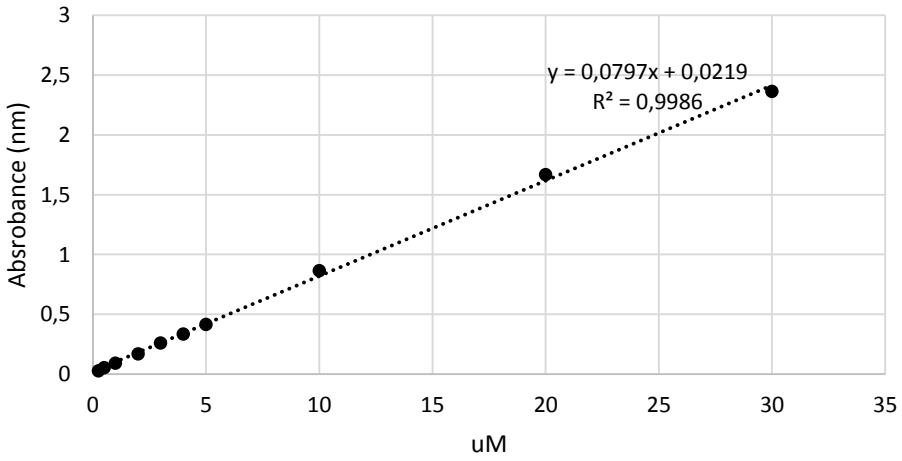


**Figure A.5 -** Calibration curve of resveratrol.